TABLE 1 Patient characteristics classified by disease progression

Characteristic[a]	Value for patients with:			P
	CH (n = 25)	LC (n = 29)	HCC (n = 25)	
No. male/female	14/11	10/19	12/13	0.278
Age (yr) (mean ± SD)	63.4 ± 14.6	66.5 ± 9.2	68.4 ± 8.2	0.539
Platelets (10^{-4}/mm^3) (mean ± SD)	16.1 ± 4.7	9.8 ± 3.9	11.1 ± 5.1	<0.001
Albumin (g/dl) (mean ± SD)	4.4 ± 0.3	3.9 ± 0.6	3.5 ± 0.5	<0.001
γ-GTP (IU/liter) (median [range])	53.5 (12–230)	38.0 (12–108)	40.8 (15–110)	0.845
T. chol. (mg/dl) (mean ± SD)	161 ± 28	148 ± 30	140 ± 28	0.053
HCV RNA (kIU/ml) (median [range])	7,047 (501–19,953)	5,369 (126–25,119)	8,421 (110–25,119)	0.288
Alpha-fetoprotein (ng/ml) (median [range])	5.0 (1.1–16.5)	32.2 (1.0–252.6)	614.8 (1.9–13,418)	<0.001
AST (IU/liter) (mean ± SD)	42.4 ± 17.8	51.1 ± 23.5	59.1 ± 28.2	0.046
ALT (IU/liter) (mean ± SD)	46.6 ± 23.1	43.9 ± 29.3	60.7 ± 52.7	0.263
No. with R/(Q/H) at core aa 70[b]	19/6	12/17	8/17	0.005
No. with L/(M/C) at core aa 91[b]	17/8	19/10	15/10	0.834
No. of ISDR mutations (median [range])[b]	0.8 (0–6)	1.2 (0–7)	0.9 (0–8)	0.799
No. of IRRDR mutations (median [range])[b]	4.9 (1–10)	4.7 (2–9)	5.2 (1–12)	0.962
No. with TT/non-TT at IL28B SNP (rs8099917)	18/7	17/12	14/11	0.458
No. without/with a history of interferon therapy	14/11	16/13	15/10	0.933

[a] T. chol., total cholesterol; AST, aspartate transaminase; ALT, alanine aminotransferase.
[b] Core aa 70, core aa 91, the interferon sensitivity-determining region (ISDR), and the interferon-ribavirin resistance-determining region (IRRDR) were dominant viral sequences determined by direct sequencing.

PATIENTS AND METHODS

Patients. The subjects were 79 patients persistently infected with HCV genotype 1b who were followed up at Yamanashi University Hospital. The patients all fulfilled the following criteria: (i) they were negative for hepatitis B surface antigen; (ii) they had no other forms of hepatitis, such as primary biliary cirrhosis, autoimmune liver disease, or alcoholic liver disease; (iii) they were free of coinfection with human immunodeficiency virus; and (iv) signed consent was obtained for the study protocol. The study protocol had been approved by the Human Ethics Review Committee of Yamanashi University Hospital and conformed to the ethical guidelines of the Declaration of Helsinki.

The breakdown was as follows: 25 patients with CH, 29 with LC, and 25 with HCC. The patients' clinical backgrounds, including histories of interferon-based antiviral therapy, are shown in Table 1. Deep-sequencing analysis was performed using serum samples taken at the most recent visit from patients with chronic hepatitis or liver cirrhosis and at the first diagnosis of HCC from patients with HCC. A direct-sequencing method, which determines the dominant viral sequence, was performed as described previously (9) to determine the dominant viral sequences of the core region, the interferon sensitivity-determining region (ISDR), and the interferon-ribavirin resistance-determining region (IRRDR) from the serum of each patient.

Deep sequencing. Deep sequencing of the viral core region was performed for each of 79 patients. Briefly, RNA was extracted from the stored sera of these patients and was reverse transcribed to cDNA. Then two-step nested PCR was carried out with primers specific for the core region of the HCV genome (23). The primers for the second-round PCR had barcodes attached, were 10 nucleotides (nt) long, and differed for each sample, so that PCR products from each sample were identifiable (see Table S1 in the supplemental material). After the band densities of the PCR products were quantified using a Bioanalyzer (Agilent Technologies, Palo Alto, CA), the concentrations of the samples were adjusted to a common value, and pooled samples were prepared. Libraries were then subjected to emulsion PCR, the enriched DNA beads loaded onto a picotiter plate, and pyrosequencing carried out with a Roche GS Junior/454 sequencing system using titanium chemistry (Roche, Branford, CT). In order to determine the error rate of the procedure, deep sequencing was carried out under similar conditions with a plasmid containing a cloned HCV sequence (pCV-J4L6S) (24). Amplicon Variant Analyzer software, version 2.5p1 (Roche), was used for analysis.

A dominant sequence of the core region for each patient was deposited in GenBank. Although the study amplified 499 nucleotides, from the 25th to the 523rd nucleotide of the core region, by PCR (Fig. 1), information for only 459 of the 499 nucleotides was uploaded for each patient, since some minor PCR amplicons obtained by deep sequencing did not include the full 499 nucleotides.

Phylogenetic tree analysis. Phylogenetic trees were constructed from the sequences by using the neighbor-joining method with BioEdit and MEGA5.05, and bootstrapping was performed with 1,000 replicates (25). In constructing phylogenetic trees, the three bases of the core codon 70 were removed in the analysis of all trees, since the mutation rate of other parts of the core region is known to be rather low, and it was possible that the influence of the core aa 70 mutations might be overestimated in the phylogenetic trees. In addition, using genetic distance data obtained from the phylogenetic analysis, the genetic distances between every two HCVs with core aa 70R, between every two HCVs with a residue other than R at core aa 70 (core aa 70non-R), and between every two HCVs with different residues at core aa 70 (one HCV with R and one with a non-R residue) were also compared statistically in order to reveal the genetic associations among those HCV core subgroups.

Statistical analysis. Statistical differences in the parameters, including all available patients' demographic, biochemical, hematological, virological, and SNP data in the three groups (CH, LC, and HCC), were determined using the Kruskal-Wallis test. The Mann-Whitney U test was used for statistical differences in numerical variables between two groups. Trends for categorical data

Downloaded from http://jvi.asm.org/ on January 21, 2014 by Kohji Moriishi

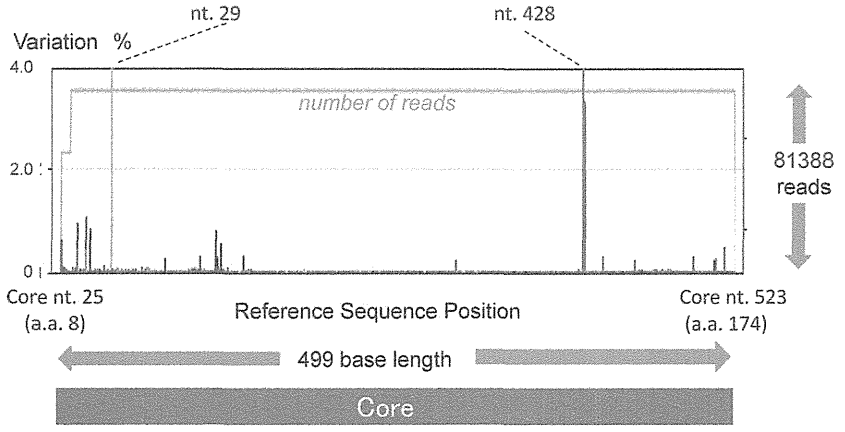

FIG 1 The core region of pCV-J4L6S (genotype 1b) from the 25th to the 523rd nucleotide, and from the 9th to the 174th codon, was subjected to deep sequencing, and the background error rate of pyrosequencing was calculated. In order to show rare background errors, those errors with low percentages are magnified.

were evaluated using the Cochran-Armitage trend test. All *P* values of <0.05 by the two-tailed test were considered significant in comparisons of genetic distances.

Nucleotide sequence accession numbers. The dominant sequences of the core regions from the patient samples have been deposited in GenBank under accession numbers AB822372.1 to AB822459.1.

RESULTS

Calculation of background errors in deep sequencing. First, the background error rate of pyrosequencing was calculated with a plasmid containing a cloned HCV sequence (pCV-J4L6S). Figure 1 shows the results of deep sequencing from the 25th to the 523rd nucleotide of the core region (499 nt) in pCV-J4L6S. Among 81,388 reads, each 499 nt long, the maximum error rate was 99.14% at the 428th base, and the next highest error rate was 64.17% at the 29th base. A six-C homopolymer region ending at the 428th base was read as a five-C homopolymer and a five-A homopolymer region ending at the 29th base was read as a four-A homopolymer in most of the obtained sequences; these homopolymer sequences are a weak point of pyrosequencing (26, 27).

A base appearing six times consecutively was the longest sequence of identical repeated nucleotides and was found only at the 428th nt position in the core region of pCV-J4L6S. Five consecutive bases were found at two sites (the 336th and 436th nt) in addition to the 29th nt position, but this error (i.e., the miscounting of homopolymer length) occurred only at the 29th base closest to the end of the sequence. Excluding the 428th and 29th nt positions, the error rate was ~1% or lower, as shown in Fig. 1. There was no single nucleotide error in the codons for aa 70 and aa 91in the repeated control experiments. From repeated deep sequencing of the plasmid, the overall nucleotide error rate was calculated as 0.092 ± 0.005 (mean ± standard deviation [SD])/base. Based on this analysis, a mixture of bases detectable above the background error of 0.102% (mean background error rate + 2 SDs) was defined as a real mixture.

Baseline characteristics. The baseline characteristics of the 79 patients are shown in Table 1. The values for viral factors core aa 70 and aa 91, NS5A-ISDR, and NS5A-IRRDR are the results of the direct-sequencing study. As shown in Table 1, the results for the variables platelets, albumin, alpha-fetoprotein, and core aa 70 differed significantly according to disease progression. On the other hand, no difference was observed in core aa 91 and IL28B SNP (rs8099917) according to disease progression.

Quasispecies nature of core amino acid 70 and disease progression. Deep sequencing of the core region was carried out with a variety of clinical samples. Simultaneous analysis was carried out using the barcoded primers, and approximately 950 reads were obtained per sample (Table 2). When the analysis was focused on core aa 70, the proportion of non-R (Q/H) sequences increased as disease severity advanced from CH to LC to HCC, as shown in Fig. 2A and Table 3 ($P = 0.018$). When a mixture of 0.102% or more was defined as a real mixture, deep sequencing showed the presence of a mixture at core aa 70 in 71 of the 79 patients (89.9%).

The relationship between disease progression and the occurrence of a quasispecies was also analyzed at the codon for core aa 91, which has also been reported to be associated with the outcomes of IFN therapy and the occurrence of HCC. As with core aa 70, a quasispecies was recognized at this site, and mixtures were observed in most patients. However, in contrast to the core aa 70 codon, there was no clear relationship with disease progression (Fig. 2B and Table 3).

Figure 2C and D show the correlation between mixtures in the core aa 70 and 91 regions and IL28B SNPs. As shown in Fig. 2C and Table 4, the proportion of mutations in the core aa 70 codon was highly dependent on the IL28B SNP (*P*, <0.005 [Table 4]). Such a relationship was also found between the proportion of mutations in core aa 91 and IL28B SNPs (Fig. 2D and Table 4), although its significance was rather weaker (*P*, 0.010).

TABLE 2 Amplicon read numbers obtained by deep sequencing of samples from 79 patients

Group	No. of patients	Total no. of reads	Avg no. of reads ± SD (range)/sample
CH	25	22,365	894.6 ± 222.8 (367–1,486)
LC	29	28,537	982.5 ± 258.1 (660–1,528)
HCC	25	24,284	971.4 ± 242.5 (405–1,749)
Total	79	75,186	951.7 ± 240.9 (367–1,749)

Downloaded from http://jvi.asm.org/ on January 21, 2014 by Kohji Moriishi

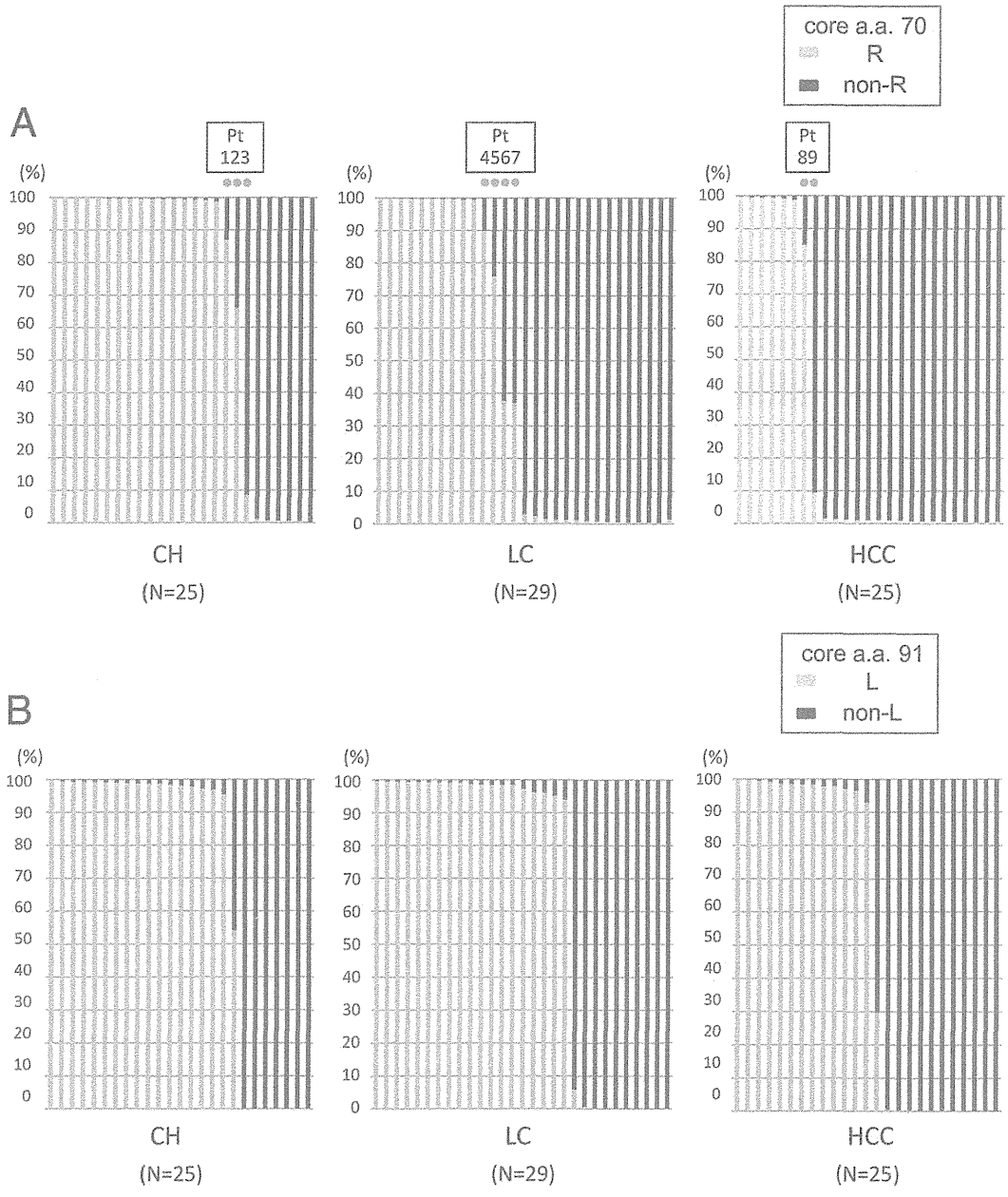

FIG 2 The core regions of the HCV genomes from 79 patients persistently infected with HCV genotype 1b (25 patients with chronic hepatitis [CH], 29 with liver cirrhosis [LC], and 25 with hepatocellular carcinoma [HCC]) were subjected to deep sequencing. Each bar represents the result for a single patient. At the specific locations of core aa 70 and aa 91, no single nucleotide mutation was observed in the previous control plasmid experiment. (A) Disease stages and percentages of mutations at core aa 70. Nine dots indicate the nine patients with a high mixture rate (between 5% and 95%) at core aa 70 (R and non-R). (B) Disease stages and percentages of mutations at core aa 91. (C) IL28B SNP and percentages of mutations at core aa 70. (D) IL28B SNP and percentages of mutations at core aa 91.

Since direct sequencing has also shown an association of several sites other than core aa 70 and 91 with the occurrence of HCC (6), those sites were also investigated for such an association. However, there was no clear relationship between these sites and disease progression, except for G209A (core aa R70Q) (see Fig. S1 and Table S2 in the supplemental material).

Phylogenetic tree analysis of HCV core region focusing on the core aa 70 residue. Because it was clear that the core aa 70 quasispecies state was significantly associated with disease progression, our next interest was to determine how this single hot spot is correlated with the remainder of the (almost-entire) core region. Therefore, phylogenetic tree analysis was performed, and genetic distances among aa 70-associated core sequences were also compared statistically. In constructing all phylogenetic trees, the three bases of the core 70 codon were removed, since the mutation rate of other parts of the core region is known to be rather low, and it was possible that the influence of the core aa 70 mutations might be overestimated in the phylogenetic trees.

At first, to determine the associations among the remainder of the core sequences across different patients, a phylogenetic tree was constructed for all 79 patients using dominant core sequences obtained from each patient. In constructing the tree, two domi-

Downloaded from http://jvi.asm.org/ on January 21, 2014 by Kohji Moriishi

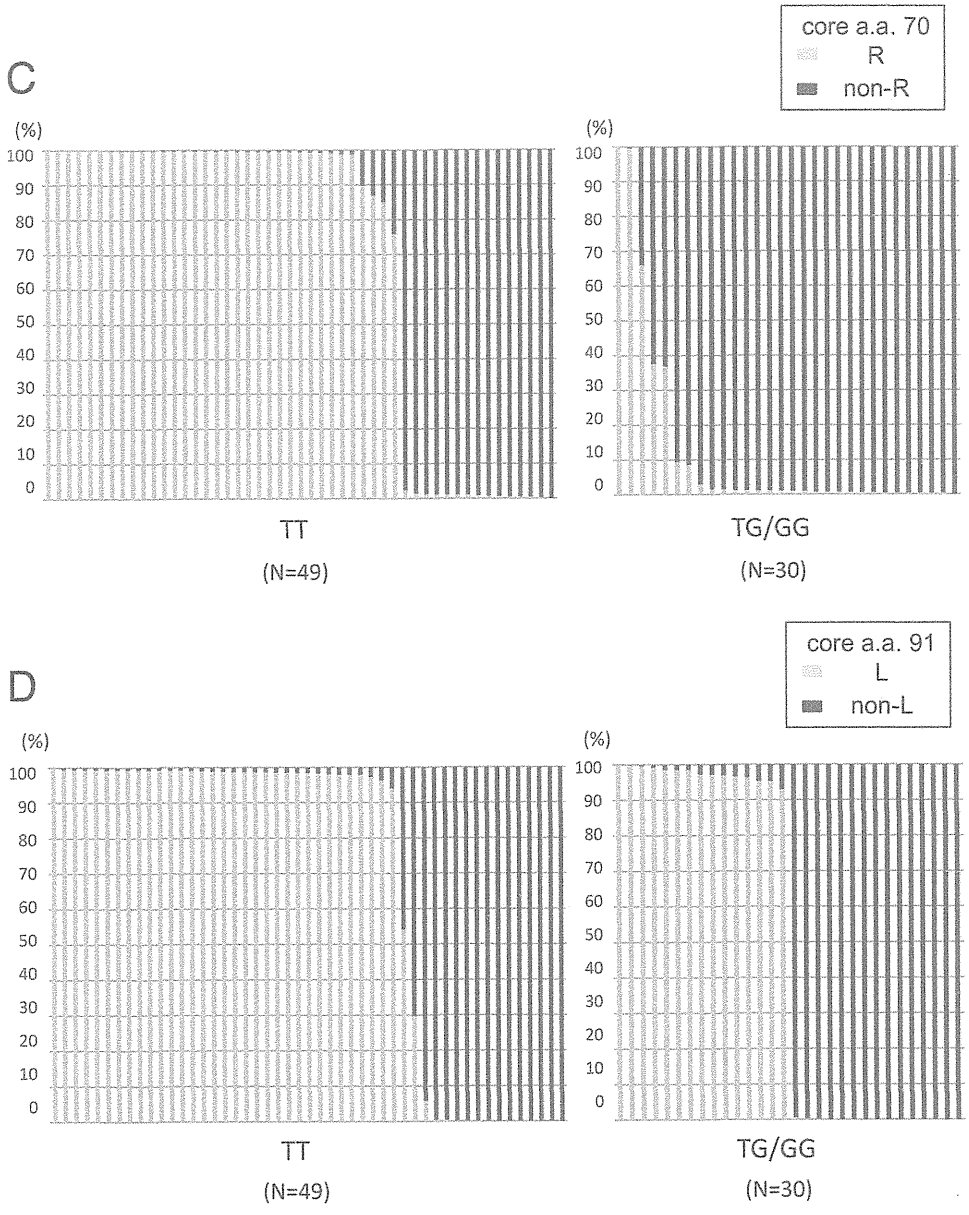

FIG 2 continued

nant sequences (the dominant core sequence in isolates with aa 70R and the dominant core sequence in isolates with aa 70non-R) were included in the analysis for each of the nine patients with high mixture rates (5% or more) of R and non-R at core aa 70 (Fig. 2A), while one dominant sequence each was included for other patients. As shown in Fig. 3A and Table 5, genetic distances calculated between every two core sequences with aa 70R (R-R) were significantly larger than those between two core sequences with aa 70non-R (non-R–non-R) or those between a

TABLE 3 Correlation between quasispecies composition and disease progression

Patient group (*n*)	Median % (range) with:	
	R at core aa 70[a]	L at core aa 91[b]
CH (25)	70.35 (0.00–100.00)	69.12 (0.00–99.40)
LC (29)	43.22 (0.24–100.00)	64.54 (0.00–99.50)
HCC (25)	28.20 (0.00–99.80)	52.23 (0.00–100.00)

[a] *P*, 0.018.
[b] *P*, 0.630.

TABLE 4 Correlation between quasispecies composition and IL28B SNP rs8099917

Group (sequence at IL28B SNP rs8099917)	Median % (range) with:	
	R at core aa 70[a]	L at core aa 91[b]
TT (*n* = 49)	68.15 (0.00–100.00)	68.24 (0.00–100.00)
TG/GG (*n* = 30)	12.64 (0.00–100.00)	48.76 (0.00–100.00)

[a] *P*, <0.005.
[b] *P*, 0.010.

Downloaded from http://jvi.asm.org/ on January 21, 2014 by Kohji Moriishi

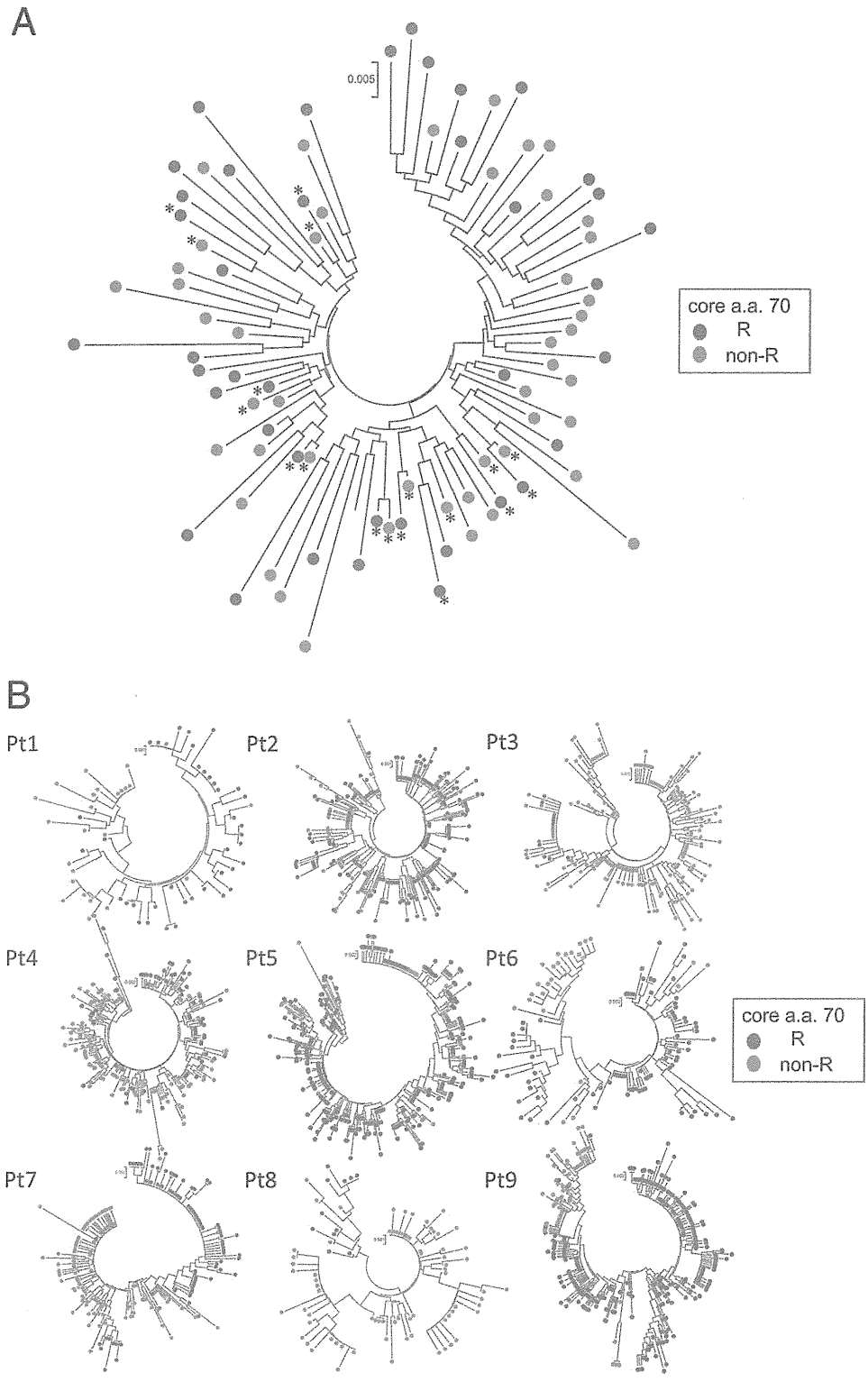

FIG 3 Phylogenetic trees were constructed using core sequences covering almost the entire core region. In the construction of those trees, the three bases of the core 70 codon were removed in the analysis of all 79 patients. Branches with core aa 70R are indicated by blue circles, while those with core aa 70non-R are indicated by pink circles. (A) Phylogenetic trees were constructed for all 79 patients by using dominant core sequences obtained from each patient. In the construction of the tree, two dominant sequences (a dominant core sequence in isolates with aa 70R and a dominant core sequence in isolates with aa 70non-R) were included in the analysis for each of the nine patients with high mixture rates (5% or more) of R and non-R at core aa 70 (Fig. 2A), while one dominant sequence each was included for other patients. (B) A phylogenetic tree of the core region was constructed for each patient with a high mixture rate (5% or more) of core aa 70R and core aa 70non-R. A total of nine patients were included in this analysis (patients 1 to 3 had CH; patients 4 to 7 had LC; and patients 9 and 10 had HCC). Pt, patient.

Downloaded from http://jvi.asm.org/ on January 21, 2014 by Kohji Moriishi

TABLE 5 Comparison of genetic distances among core subgroups related to aa 70 residues

Patient(s)[a]	Genetic distance (mean ± SD) between two core sequences[b]			Comparison of genetic distance measurements					
				Non-R–R vs non-R–non-R		Non-R–R vs R-R		Non-R–non-R vs R-R	
	Non-R–non-R	Non-R–R	R-R	Larger genetic distance	*P*	Larger genetic distance	*P*	Larger genetic distance	*P*
All (n = 79)	0.0349 ± 0.0101	0.0379 ± 0.0109	0.0401 ± 0.0113	Non-R–R	<0.001	R-R	<0.001	R-R	<0.001
CH									
Pt 1	0.0086 ± 0.0042	0.0098 ± 0.0037	0.0064 ± 0.0042	Non-R–R	<0.001	Non-R–R	<0.001	Non-R–non-R	<0.001
Pt 2	0.0097 ± 0.0048	0.0104 ± 0.0041	0.0087 ± 0.0038	Non-R–R	<0.001	Non-R–R	<0.001	Non-R–non-R	0.009
Pt 3	0.0107 ± 0.0058	0.0137 ± 0.0050	0.0034 ± 0.0022	Non-R–R	<0.001	Non-R–R	<0.001	Non-R–non-R	<0.001
LC									
Pt 4	0.0078 ± 0.0036	0.0103 ± 0.0038	0.0053 ± 0.0029	Non-R–R	<0.001	Non-R–R	<0.001	Non-R–non-R	<0.001
Pt 5	0.0118 ± 0.0090	0.0232 ± 0.0085	0.0159 ± 0.0170	Non-R–R	<0.001	Non-R–R	<0.001	No difference	0.991
Pt 6	0.0115 ± 0.0057	0.0121 ± 0.0055	0.0108 ± 0.0056	Non-R–R	<0.001	Non-R–R	<0.001	Non-R–non-R	<0.001
Pt 7	0.0141 ± 0.0085	0.0146 ± 0.0070	0.0136 ± 0.0067	Non-R–R	0.002	Non-R–R	<0.001	Non-R–non-R	<0.001
HCC									
Pt 8	0.0124 ± 0.0063	0.0225 ± 0.0060	0.0181 ± 0.0094	Non-R–R	<0.001	Non-R–R	<0.001	R-R	<0.001
Pt 9	0.0082 ± 0.0042	0.0162 ± 0.0047	0.0078 ± 0.0050	Non-R–R	<0.001	Non-R–R	<0.001	Non-R–non-R	<0.001

[a] Pt, patient.

[b] Non-R–non-R, comparison of two core sequences with residues other than R at aa 70; Non-R–R, comparison of a core sequence with a residue other than R at aa 70 and a core sequence with aa 70R; R-R, comparison of two core sequences with aa 70R. Genetic distances were calculated for all patients by using dominant sequences and for a single patient by using quasispecies sequences.

core sequence with aa 70R and a core sequence with aa 70non-R (non-R–R), demonstrating that core sequences with aa 70R were heterogeneous, while core sequences with aa 70non-R were homogeneous.

Next, to determine the association of the remainder of the core sequences in a single patient, phylogenetic trees were also constructed for each of the nine patients with high mixture rates (5% or more) of R and non-R residues at core aa 70 (Fig. 3B). As shown in Fig. 3B, HCV isolates with core aa 70R and those with core aa 70non-R formed distinctly clustered subgroups on the phylogenetic tree, according to the mutation status at core aa 70. Comparison of genetic distances also proved the finding that HCV isolates with core aa 70R and those with core aa 70non-R form distinctly clustered subgroups on the phylogenetic tree in a single patient, since genetic distances calculated between every two core sequences with aa 70R (R-R) or between every two core sequences with aa 70non-R (non-R–non-R) were significantly smaller than those between a core sequence with aa 70R and a core sequence with aa 70non-R (non-R–R). On the other hand, no significant difference was found when the genetic distance between two core sequences with aa 70non-R (non-R–non-R) and that between two core sequences with aa 70R (R-R) were compared in a single patient (Table 5).

Since the genetic relationships of the remainder of the core sequences were found to differ significantly according to the core aa 70 residue, we then investigated whether there are any common haplotypic sequences specific to each residue. In the comparison of dominant sequences in all 79 patients, most amino acid substitutions clustered in three amino acids (aa 70, aa 75, and aa 91) both in core sequences with aa 70R and in those with aa 70nonR, but no other substitutions specific to each core aa 70 residue were found (Fig. 4).

Quasispecies at core aa 70 and clinical characteristics. To clarify the association of the core aa 70 quasispecies with the clinical picture, levels of gamma-glutamyl transpeptidase (γ-GTP), albumin, platelets, and alpha-fetoprotein, as well as disease progression in the liver, were investigated for correlation with the core aa 70R/non-R mixture ratio. As shown in Fig. 5A and B, the values for these clinical parameters became significantly more abnormal as the proportion of non-R residues increased, showing that a high proportion of non-R residues at core aa 70 was significantly associated with disease severity and hepatocarcinogenesis.

DISCUSSION

This study examined, for the first time, the relationship between the progression of liver disease and the quasispecies nature of the HCV core region (already known to be associated with liver disease progression) by deep sequencing, with the focus on the core aa 70 residue. The analysis revealed that core aa 70 existed as a mixture of "mutant" Q/H (non-R) and "wild-type" R residues in most of the patients and that the proportion of mutant residues increased as liver disease advanced to LC and HCC. Meanwhile, phylogenetic analysis showed that the viral sequences of the almost-entire core region differed genetically depending on the status of core aa 70.

Before starting the analysis, we verified the rate of background error associated with the process of pyrosequencing by analyzing the control plasmid pCV-J4L6S (Fig. 1). Homopolymers of repeated bases, a weak point of pyrosequencing, were generated at two sites, with the same base appearing five and six times. The overall mutation rate at other sites was 0.092% ± 0.005%, and a mutation rate of 0.102% (mean + 2 SDs) or higher was defined as significant in the analysis, in order to avoid detecting background errors.

We focused our analysis on the quasispecies state of core aa 70,

Downloaded from http://jvi.asm.org/ on January 21, 2014 by Kohji Moriishi

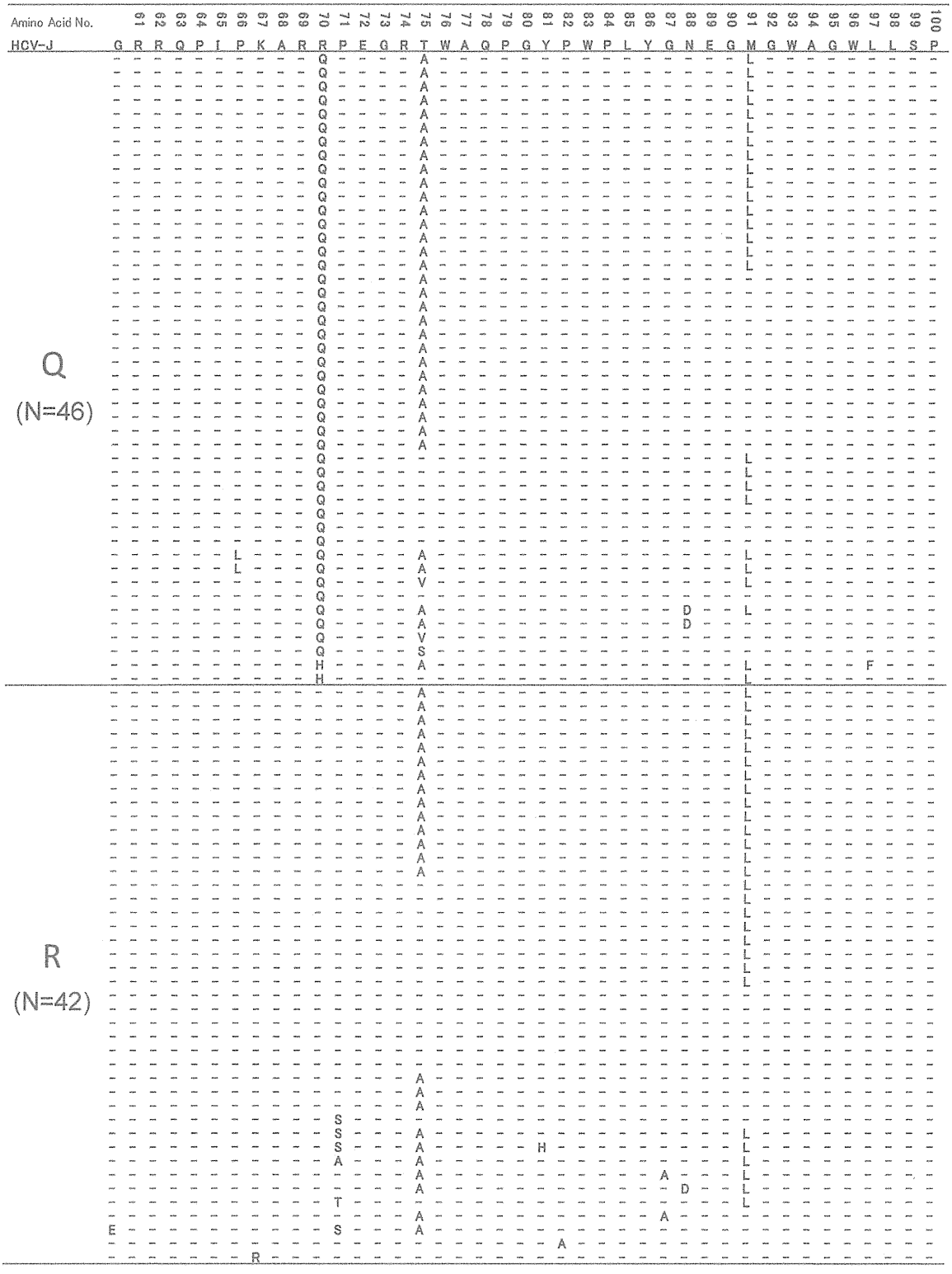

FIG 4 Dominant core amino acid haplotypic sequences dependent on the core aa 70 residues are given for all 79 patients. Two dominant sequences (a dominant core sequence in isolates with aa 70R and a dominant core sequence in isolates with aa 70non-R) were included for each of nine patients with high mixture rates (5% or more) of R and non-R at core aa 70, while one dominant sequence each was included for other patients. Therefore, a total of 88 haplotypic sequences are shown here. Since most amino acid mutations were observed in the limited core region, only that part of the core sequence is shown. The HCV-J isolate is used as the reference sequence for the core region.

Downloaded from http://jvi.asm.org/ on January 21, 2014 by Kohji Moriishi

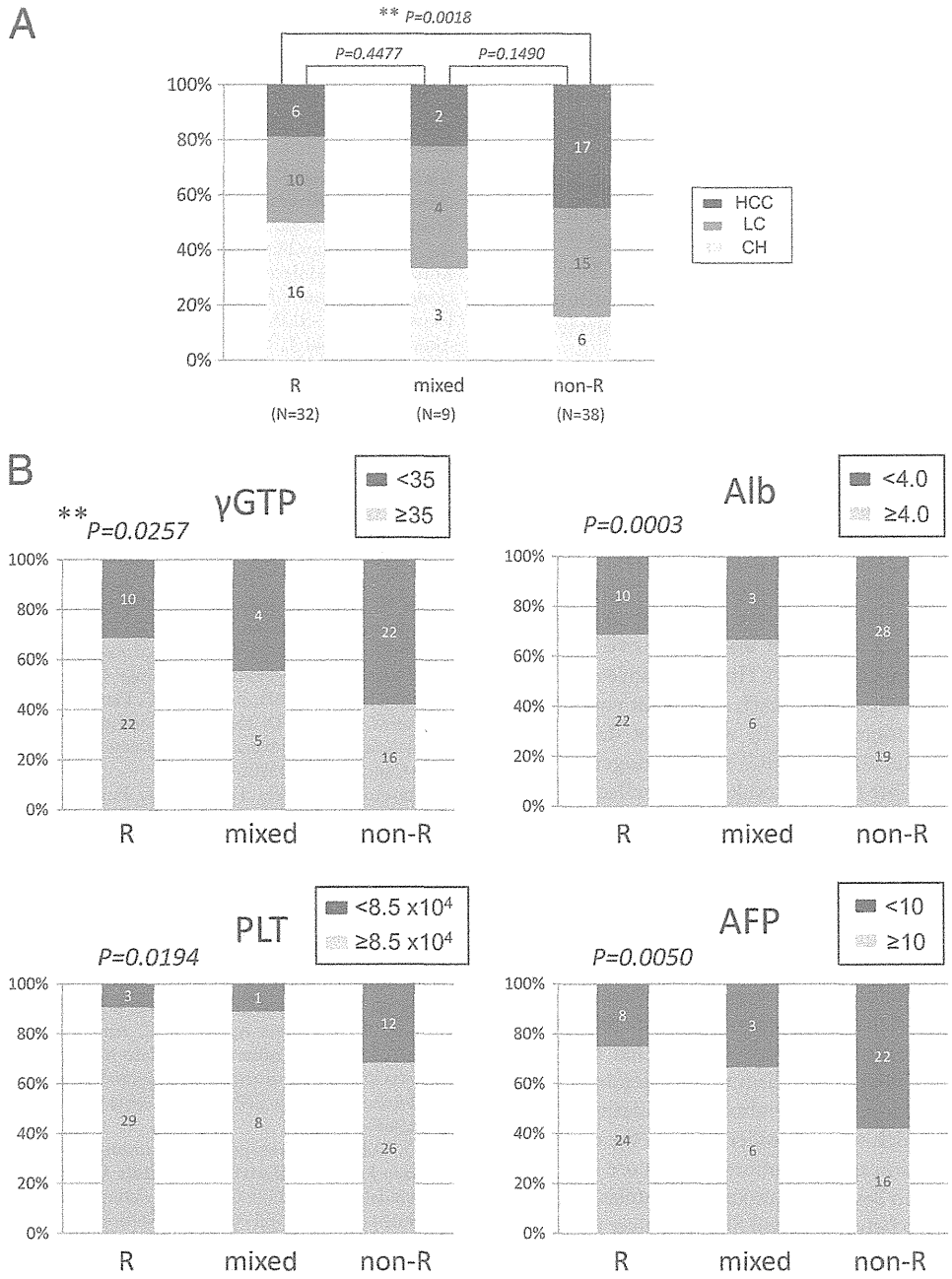

FIG 5 The advance of liver disease (A) and the levels of γ-GTP, albumin (Alb), platelets (PLT), and alpha-fetoprotein (AFP) (B) were investigated for correlation with the ratio of R to non-R at core aa 70. Results for R/R + non-R ratios of ≥95% (R), ≥5% and <95% (mixed), and <5% (non-R) are shown. **, Cochran-Armitage analysis.

because the presence of a quasispecies was expected at this position, considering reports by previous studies of its association with liver disease progression and the frequent observation of time-dependent changes (8, 9). R and non-R residues were mixed in 89.9% of the 79 patients examined in this study, indicating that the absence of a mixture was rare. Furthermore, the percentage of total isolates encoding non-R residues at this position showed a relationship with the advance of chronic liver disease, as shown in Fig. 2A and Table 3. Therefore, with regard to the relationship between the advance of liver disease and core aa 70, it may be accurate to say that a change in the ratio of amino acids at core aa 70, rather than mutation of core aa 70, was related to the advance of liver disease.

Because information for almost the entire core region was obtained from each patient, our next interest was to determine whether core aa 70 is associated with other viral regions. In other words, we sought to determine whether HCVs with core aa 70R and HCVs with core aa 70non-R are phylogenetically distinct variants. To clarify the issue, phylogenetic tree analysis using dominant sequences for the (almost-entire) core regions from all 79 patients was performed at first. This analysis disclosed, after the calculation of genetic distances, that core sequences with aa

Downloaded from http://jvi.asm.org/ on January 21, 2014 by Kohji Moriishi

70non-R were significantly more homogeneous than those with aa 70R, demonstrating that the hot spot core aa 70 residue is significantly associated with the remainder of the core sequence. Although the underlying mechanism is unclear, we speculated that the close correlation between core aa 70 residues and IL28B SNPs might have contributed to the result. That is, since endogenous IFN levels are known to be upregulated in patients with IL28B minor types (TG/GG) relative to those in patients with the IL28B major type (TT) in its natural state (28), it is possible that HCVs with core aa 70non-R, which are closely linked to IL28B TG/GG, are under strong antiviral pressure induced by IFN, resulting in the selection of more-homogeneous HCVs, which can survive in such an environment.

Considering this possibility, we proceeded to perform phylogenetic analyses of core sequences in single patients with high-percentage mixtures (5% or more) of R and non-R residues at core aa 70 by using deep-sequencing data, since the influence of endogenous IFNs was considered equal for all HCV isolates in a single patient. The deep-sequencing data showed that the genetic heterogeneity of core sequences in a single patient did not differ according to the core aa 70 residue but that core sequences formed distinct subgroups on the phylogenetic tree according to the core aa 70 residue (Fig. 3B), and this result was also proved by the calculation of genetic distances (Table 5). However, since no common haplotypic sequences specific to each residue at core aa 70 were found across the patients (Fig. 4), we cannot determine whether core aa 70R and aa 70non-R HCVs are phylogenetically distinct variants. It is possible that the result simply reflects a major evolutional event of core aa 70 mutations followed by derivative variants; however, extension of the investigation and analysis to viral regions beyond the core region might reveal such associations. However, due to the technical limitations of second-generation sequencers, deep-sequencing analysis of the long amplicon is difficult, and new technology is needed.

With regard to the mechanism underlying the relationship between the core protein and disease progression and hepatocarcinogenesis, a study using transgenic mice showed that the core protein induces HCC (29). Fat metabolism was accelerated in the liver, leading to inflammation, iron metabolism, oxidative stress, and insulin resistance, which were considered to be the carcinogenic factors (30–32). Clinically, mutation of the core and the concentration of γ-GTP in serum, a marker of steatosis, are related, and the relationship between IL28B SNP and liver steatosis or γ-GTP has been elucidated (33). In this study, moreover, we have confirmed the correlation between the core aa 70 mixture ratio, determined by deep-sequencing analysis, and clinical parameters reflecting disease progression, illustrating the significant association of core aa 70 with disease progression (Fig. 5A and B).

In conclusion, the quasispecies state of the core region was analyzed by deep sequencing. It was found that the status of the quasispecies was closely related to the advance of HCV-associated liver disease. In order to understand the mechanism of hepatocarcinogenesis, it is desirable to elucidate pathogenesis further by detailed examination of the quasispecies of the HCV core gene.

ACKNOWLEDGMENTS

Nobuyuki Enomoto received research funding from MSD (Tokyo, Japan) and Roche (Tokyo, Japan).

This study was supported in part by grants-in-aid from the Ministry of Education, Science, Sports and Culture of Japan (grants 23390195, 23791404, 24590964, and 24590965) and in part by grants-in-aid from the Ministry of Health, Labour, and Welfare of Japan (H23-kanen-001, H23-kanen-004, H23-kanen-006, H24-kanen-002, H24-kanen-004, and H25-kanen-006).

REFERENCES

1. Niederau C, Lange S, Heintges T, Erhardt A, Buschkamp M, Hurter D, Nawrocki M, Kruska L, Hensel F, Petry W, Haussinger D. 1998. Prognosis of chronic hepatitis C: results of a large, prospective cohort study. Hepatology 28:1687–1695.
2. Koike K. 2005. Molecular basis of hepatitis C virus-associated hepatocarcinogenesis: lessons from animal model studies. Clin. Gastroenterol. Hepatol. 3:S132–S135.
3. Akuta N, Suzuki F, Sezaki H, Suzuki Y, Hosaka T, Someya T, Kobayashi M, Saitoh S, Watahiki S, Sato J, Matsuda M, Arase Y, Ikeda K, Kumada H. 2005. Association of amino acid substitution pattern in core protein of hepatitis C virus genotype 1b high viral load and non-virological response to interferon-ribavirin combination therapy. Intervirology 48:372–380.
4. Akuta N, Suzuki F, Hirakawa M, Kawamura Y, Sezaki H, Suzuki Y, Hosaka T, Kobayashi M, Saitoh S, Arase Y, Ikeda K, Kumada H. 2011. Amino acid substitutions in hepatitis C virus core region predict hepatocarcinogenesis following eradication of HCV RNA by antiviral therapy. J. Med. Virol. 83:1016–1022.
5. Akuta N, Suzuki F, Kawamura Y, Yatsuji H, Sezaki H, Suzuki Y, Hosaka T, Kobayashi M, Arase Y, Ikeda K, Kumada H. 2007. Amino acid substitutions in the hepatitis C virus core region are the important predictor of hepatocarcinogenesis. Hepatology 46:1357–1364.
6. Fishman SL, Factor SH, Balestrieri C, Fan X, Dibisceglie AM, Desai SM, Benson G, Branch AD. 2009. Mutations in the hepatitis C virus core gene are associated with advanced liver disease and hepatocellular carcinoma. Clin. Cancer Res. 15:3205–3213.
7. Nakamoto S, Imazeki F, Fukai K, Fujiwara K, Arai M, Kanda T, Yonemitsu Y, Yokosuka O. 2010. Association between mutations in the core region of hepatitis C virus genotype 1 and hepatocellular carcinoma development. J. Hepatol. 52:72–78.
8. Akuta N, Suzuki F, Seko Y, Kawamura Y, Sezaki H, Suzuki Y, Hosaka T, Kobayashi M, Hara T, Saitoh S, Arase Y, Ikeda K, Kumada H. 2012. Complicated relationships of amino acid substitution in hepatitis C virus core region and IL28B genotype influencing hepatocarcinogenesis. Hepatology 56:2134–2141.
9. Miura M, Maekawa S, Kadokura M, Sueki R, Komase K, Shindo H, Ohmori T, Kanayama A, Shindo K, Amemiya F, Nakayama Y, Kitamura T, Uetake T, Inoue T, Sakamoto M, Okada S, Enomoto N. 2012. Analysis of viral amino acids sequences and the IL28B SNP influencing the development of hepatocellular carcinoma in chronic hepatitis C. Hepatol. Int. 6:386–396.
10. Ge D, Fellay J, Thompson AJ, Simon JS, Shianna KV, Urban TJ, Heinzen EL, Qiu P, Bertelsen AH, Muir AJ, Sulkowski M, McHutchison JG, Goldstein DB. 2009. Genetic variation in IL28B predicts hepatitis C treatment-induced viral clearance. Nature 461:399–401.
11. Rauch A, Kutalik Z, Descombes P, Cai T, Di Iulio J, Mueller T, Bochud M, Battegay M, Bernasconi E, Borovicka J, Colombo S, Cerny A, Dufour JF, Furrer H, Gunthard HF, Heim M, Hirschel B, Malinverni R, Moradpour D, Mullhaupt B, Witteck A, Beckmann JS, Berg T, Bergmann S, Negro F, Telenti A, Bochud PY. 2010. Genetic variation in *IL28B* is associated with chronic hepatitis C and treatment failure: a genome-wide association study. Gastroenterology 138:1338–1345.e7.
12. Suppiah V, Moldovan M, Ahlenstiel G, Berg T, Weltman M, Abate ML, Bassendine M, Spengler U, Dore GJ, Powell E, Riordan S, Sheridan D, Smedile A, Fragomeli V, Muller T, Bahlo M, Stewart GJ, Booth DR, George J. 2009. IL28B is associated with response to chronic hepatitis C interferon-alpha and ribavirin therapy. Nat. Genet. 41:1100–1104.
13. Tanaka Y, Nishida N, Sugiyama M, Kurosaki M, Matsuura K, Sakamoto N, Nakagawa M, Korenaga M, Hino K, Hige S, Ito Y, Mita E, Tanaka E, Mochida S, Murawaki Y, Honda M, Sakai A, Hiasa Y, Nishiguchi S, Koike A, Sakaida I, Imamura M, Ito K, Yano K, Masaki N, Sugauchi F, Izumi N, Tokunaga K, Mizokami M. 2009. Genome-wide association of IL28B with response to pegylated interferon-alpha and ribavirin therapy for chronic hepatitis C. Nat. Genet. 41:1105–1109.
14. Bochud PY, Bibert S, Kutalik Z, Patin E, Guergnon J, Nalpas B, Goossens N, Kuske L, Mullhaupt B, Gerlach T, Heim MH, Moradpour

Downloaded from http://jvi.asm.org/ on January 21, 2014 by Kohji Moriishi

D, Cerny A, Malinverni R, Regenass S, Dollenmaier G, Hirsch H, Martinetti G, Gorgiewski M, Bourliere M, Poynard T, Theodorou I, Abel L, Pol S, Dufour JF, Negro F. 2012. IL28B alleles associated with poor hepatitis C virus (HCV) clearance protect against inflammation and fibrosis in patients infected with non-1 HCV genotypes. Hepatology 55: 384–394.
15. Fabris C, Falleti E, Cussigh A, Bitetto D, Fontanini E, Bignulin S, Cmet S, Fornasiere E, Fumolo E, Fangazio S, Cerutti A, Minisini R, Pirisi M, Toniutto P. 2011. IL-28B rs12979860 C/T allele distribution in patients with liver cirrhosis: role in the course of chronic viral hepatitis and the development of HCC. J. Hepatol. 54:716–722.
16. Joshita S, Umemura T, Katsuyama Y, Ichikawa Y, Kimura T, Morita S, Kamijo A, Komatsu M, Ichijo T, Matsumoto A, Yoshizawa K, Kamijo N, Ota M, Tanaka E. 2012. Association of IL28B gene polymorphism with development of hepatocellular carcinoma in Japanese patients with chronic hepatitis C virus infection. Hum. Immunol. 73:298–300.
17. Marabita F, Aghemo A, De Nicola S, Rumi MG, Cheroni C, Scavelli R, Crimi M, Soffredini R, Abrignani S, De Francesco R, Colombo M. 2011. Genetic variation in the interleukin-28B gene is not associated with fibrosis progression in patients with chronic hepatitis C and known date of infection. Hepatology 54:1127–1134.
18. Pawlotsky JM. 2006. Hepatitis C virus population dynamics during infection. Curr. Top. Microbiol. Immunol. 299:261–284.
19. Hiraga N, Imamura M, Abe H, Hayes CN, Kono T, Onishi M, Tsuge M, Takahashi S, Ochi H, Iwao E, Kamiya N, Yamada I, Tateno C, Yoshizato K, Matsui H, Kanai A, Inaba T, Tanaka S, Chayama K. 2011. Rapid emergence of telaprevir resistant hepatitis C virus strain from wild-type clone in vivo. Hepatology 54:781–788.
20. Nasu A, Marusawa H, Ueda Y, Nishijima N, Takahashi K, Osaki Y, Yamashita Y, Inokuma T, Tamada T, Fujiwara T, Sato F, Shimizu K, Chiba T. 2011. Genetic heterogeneity of hepatitis C virus in association with antiviral therapy determined by ultra-deep sequencing. PLoS One 6:e24907. doi:10.1371/journal.pone.0024907.
21. Verbinnen T, Van Marck H, Vandenbroucke I, Vijgen L, Claes M, Lin TI, Simmen K, Neyts J, Fanning G, Lenz O. 2010. Tracking the evolution of multiple *in vitro* hepatitis C virus replicon variants under protease inhibitor selection pressure by 454 deep sequencing. J. Virol. 84:11124–11133.
22. Wang GP, Sherrill-Mix SA, Chang KM, Quince C, Bushman FD. 2010. Hepatitis C virus transmission bottlenecks analyzed by deep sequencing. J. Virol. 84:6218–6228.
23. Nagayama K, Kurosaki M, Enomoto N, Maekawa SY, Miyasaka Y, Tazawa J, Izumi N, Marumo F, Sato C. 1999. Time-related changes in full-length hepatitis C virus sequences and hepatitis activity. Virology 263: 244–253.
24. Gates AT, Sarisky RT, Gu B. 2004. Sequence requirements for the development of a chimeric HCV replicon system. Virus Res. 100:213–222.
25. Tamura K, Peterson D, Peterson N, Stecher G, Nei M, Kumar S. 2011. MEGA5: molecular evolutionary genetics analysis using maximum likelihood, evolutionary distance, and maximum parsimony methods. Mol. Biol. Evol. 28:2731–2739.
26. Becker EA, Burns CM, Leon EJ, Rajabojan S, Friedman R, Friedrich TC, O'Connor SL, Hughes AL. 2012. Experimental analysis of sources of error in evolutionary studies based on Roche/454 pyrosequencing of viral genomes. Genome Biol. Evol. 4:457–465.
27. Quince C, Lanzen A, Curtis TP, Davenport RJ, Hall N, Head IM, Read LF, Sloan WT. 2009. Accurate determination of microbial diversity from 454 pyrosequencing data. Nat. Methods 6:639–641.
28. Honda M, Sakai A, Yamashita T, Nakamoto Y, Mizukoshi E, Sakai Y, Nakamura M, Shirasaki T, Horimoto K, Tanaka Y, Tokunaga K, Mizokami M, Kaneko S. 2010. Hepatic ISG expression is associated with genetic variation in interleukin 28B and the outcome of IFN therapy for chronic hepatitis C. Gastroenterology 139:499–509.
29. Moriya K, Fujie H, Shintani Y, Yotsuyanagi H, Tsutsumi T, Ishibashi K, Matsuura Y, Kimura S, Miyamura T, Koike K. 1998. The core protein of hepatitis C virus induces hepatocellular carcinoma in transgenic mice. Nat. Med. 4:1065–1067.
30. Leandro G, Mangia A, Hui J, Fabris P, Rubbia-Brandt L, Colloredo G, Adinolfi LE, Asselah T, Jonsson JR, Smedile A, Terrault N, Pazienza V, Giordani MT, Giostra E, Sonzogni A, Ruggiero G, Marcellin P, Powell EE, George J, Negro F. 2006. Relationship between steatosis, inflammation, and fibrosis in chronic hepatitis C: a meta-analysis of individual patient data. Gastroenterology 130:1636–1642.
31. Nishina S, Hino K, Korenaga M, Vecchi C, Pietrangelo A, Mizukami Y, Furutani T, Sakai A, Okuda M, Hidaka I, Okita K, Sakaida I. 2008. Hepatitis C virus-induced reactive oxygen species raise hepatic iron level in mice by reducing hepcidin transcription. Gastroenterology 134:226–238.
32. Okuda M, Li K, Beard MR, Showalter LA, Scholle F, Lemon SM, Weinman SA. 2002. Mitochondrial injury, oxidative stress, and antioxidant gene expression are induced by hepatitis C virus core protein. Gastroenterology 122:366–375.
33. Abe H, Ochi H, Maekawa T, Hayes CN, Tsuge M, Miki D, Mitsui F, Hiraga N, Imamura M, Takahashi S, Ohishi W, Arihiro K, Kubo M, Nakamura Y, Chayama K. 2010. Common variation of IL28 affects γ-GTP levels and inflammation of the liver in chronically infected hepatitis C virus patients. J. Hepatol. 53:439–443.

Downloaded from http://jvi.asm.org/ on January 21, 2014 by Kohji Moriishi

Oral Administration of the CCR5 Inhibitor, Maraviroc, Blocks HIV *Ex vivo* Infection of Langerhans Cells Within the Epithelium

Journal of Investigative Dermatology accepted article preview 6 May 2013; doi:10.1038/jid.2013.215

TO THE EDITOR

Preexposure prophylaxis (PrEP) with oral administration of an antiretroviral is a potential method for preventing acquisition of HIV. A controlled trial in men who have sex with men (the iPrEx trial) showed that daily oral use of tenofovir disoproxil fumarate-emtricitabine (TDF-FTC; Truvada) reduced transmission rates by 44% (Grant *et al.*, 2010). In addition, the HIV Prevention Trial Network (HPTN) 052 trial recently confirmed that antiretroviral treatment leads to 96% reduction in transmission among HIV-negative heterosexual partners of HIV-positive individuals (Cohen *et al.*, 2011). Similar trials, however, with TDF-FTC (the FEM-PrEP trial) or TDF alone (the VOICE trial) were stopped because of poor outcomes (van der Straten *et al.*, 2012). Different results among various trials, which used identical antiretroviral regimens, could be explained by varying compliance with drug use and/or varying drug concentration and activity within the exposed tissue (Patterson *et al.*, 2011).

Langerhans cells (LCs) are $CCR5^+$ dendritic cells located within genital skin and mucosal epithelium (Lederman *et al.*, 2006). In female rhesus macaques exposed intravaginally to simian immunodeficiency virus, up to 90% of initially infected target cells were LCs (Hu *et al.*, 2000). *Ex vivo* experiments with human foreskin explants show that epidermal LCs are target cells for HIV, providing a likely explanation for why circumcision greatly reduces the probability of acquiring HIV (Ganor *et al.*, 2010). LCs also express CD4 and CCR5, but not CXCR4, within the tissue and demonstrate the distinctive characteristics of emigrating from tissue to draining lymph nodes in order to interact with T cells after contact with pathogens (Kawamura *et al.*, 2000). Indeed, epidermal LCs are readily infected *ex vivo* with R5 HIV, but not with X4 HIV, and promote high levels of infection upon interaction with cocultured $CD4^+$ T cells (Kawamura *et al.*, 2000; Ogawa *et al.*, 2013). Thus, LCs probably have an important role in disseminating HIV soon after exposure to virus.

Epidemiologic observations have found that the majority of HIV strains isolated from patients soon after initial infection are R5 HIV strains (i.e., they utilize CCR5; Lederman *et al.*, 2006). Not surprisingly, individuals with homozygous defects in *CCR5* are largely protected from sexually acquiring HIV (Lederman *et al.*, 2006). In addition, three different CCR5-binding topically applied compounds protected female macaques from sexually acquiring SHIV: the N-terminally modified chemokine analog PSC-RANTES, the small-molecule inhibitor CMPD167, and maraviroc (MVC) (Lederman *et al.*, 2006; Veazey *et al.*, 2010). In addition to topical application to vaginal mucosa, oral delivery of CMPD167 protected macaques from vaginal SHIV challenge (Veazey *et al.*, 2005). Given these data, orally administered MVC may prove to be particularly important in PrEP regimens, although its ability to prevent HIV acquisition is unknown.

In the current study, 20 healthy volunteers were randomly divided into four equal groups; they received 300 mg of MVC orally twice daily for 1, 2, 3, or 14 days. To obtain epidermal tissues, all subjects underwent suction blistering of the skin before and 2 hours after the last MVC dose. All subjects had plasma and semen collected 2 hours after their last dose. MVC concentrations in serum, semen, and epidermal tissues were determined by using the liquid chromatography– mass spectometry method, as described previously (Takahashi *et al.*, 2010). Mean concentration ± SD in the epidermis was 21.91 ± 13.80, 23.36 ± 13.28, and 31.54 ± 20.61 nM for individuals taking drug for 1, 2, or 3 days ($n = 5$ for each), respectively. MVC concentrations tended to be higher with a longer dosing period. Consistent with recent data showing high levels of MVC in genital tissue (Dumond *et al.*, 2009), these results indicate that MVC rapidly distributes into the skin at high concentrations. In addition, MVC was detected in semen of all subjects (Supplementary Figure S1 online).

To understand how HIV traverses skin and genital mucosa, an *ex vivo* model was developed whereby resident LCs within epithelial tissue explants are exposed to HIV and then allowed to emigrate from tissue, thus mimicking conditions that occur after mucosal exposure to HIV (Kawamura *et al.*, 2000; Ogawa *et al.*, 2013). In this model, although relatively few productively infected LCs are identified, these cells induce high levels of HIV infection when cocultured with resting autologous $CD4^+$ T cells (Kawamura *et al.*, 2000). In preliminary experiments, HIV infection of LCs, as well as subsequent virus transmission from emigrated LCs to cocultured $CD4^+$ T cells, was decreased in a dose-dependent manner when skin explants were pretreated with

© 2013 The Society for Investigative Dermatology

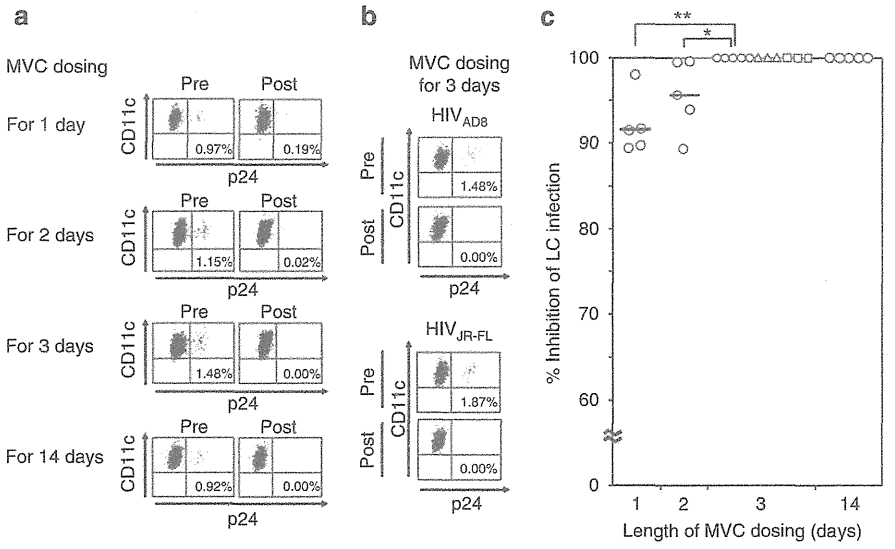

Figure 1. Oral administration of maraviroc (MVC) protects epidermal Langerhans cells (LCs) from *ex vivo* R5 HIV infection. Skin explants were isolated from healthy individuals who had received oral MVC (300 mg twice daily) for the indicated periods of time. These tissues were exposed to HIV_{Ba-L} (**a**, **c**), HIV_{AD8}, or HIV_{JR-FL} (**b**, **c**) and then cultured for 3 days. Emigrated LCs were collected and assessed for HIV infection by flow cytometry. Representative FACS analyses of CD11c and p24 mAb double-stained cells are shown (**a**, **b**). Percent MVC inhibition of LC infection with HIV_{Ba-L} (○), HIV_{AD8} (△), or HIV_{JR-FL} (□) was calculated as described in the text (**c**). $^*P<0.05$; $^{**}P<0.01$. Mean values obtained from different donors are shown as horizontal marks.

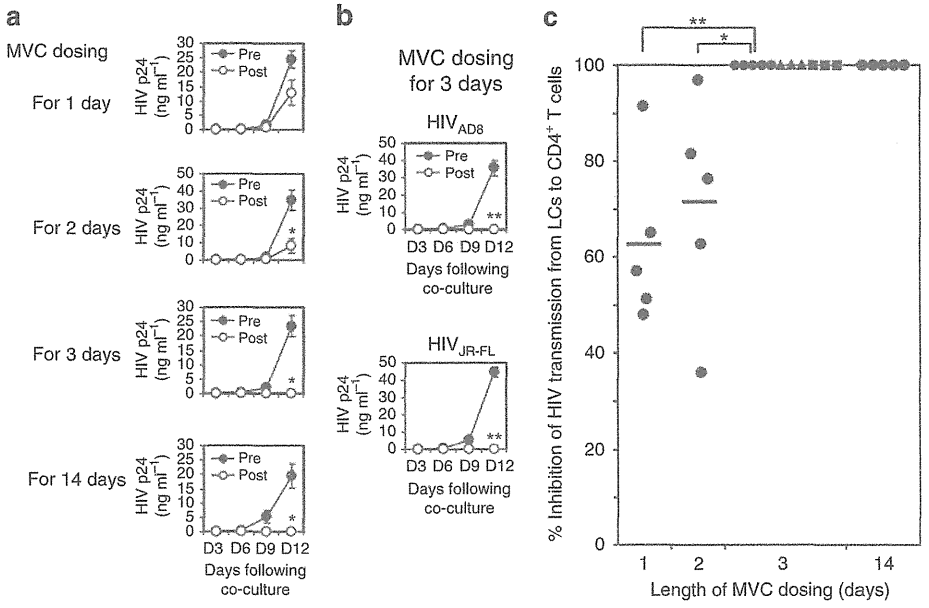

Figure 2. Oral administration of maraviroc (MVC) blocks viral transmission from HIV-exposed Langerhans cells (LCs) to cocultured CD4$^+$ T cells. Skin explants isolated from healthy individuals who had received oral MVC (300 mg twice daily) for the indicated periods of time were exposed to HIV_{Ba-L} (**a**, **c**), HIV_{AD8}, or HIV_{JR-FL} (**b**, **c**), as described in Figure 1. Emigrated LCs were cocultured with autologous CD4$^+$ T cells, and culture supernatants were assessed for p24 content by ELISA. Representative ELISA results are shown (**a**, **b**). Percent MVC inhibition of HIV_{Ba-L} (●), HIV_{AD8} (▲), or HIV_{JR-FL} (■) transmission to cocultured CD4$^+$ T cells was calculated as described in the text (**c**). $^*P<0.05$; $^{**}P<0.01$. Mean values obtained from different donors are shown as horizontal marks.

various concentrations of MVC before HIV exposure (Supplementary Figure S2 online), similar to experiments reported earlier with PSC-RANTES (Kawamura *et al.*, 2004).

Next, the epithelial tissue explants were collected from study subjects after oral treatment with MVC (Supplementary Materials and Methods online). Importantly, oral MVC pretreatment for either 1 or 2 days partially inhibited subsequent *ex vivo* HIV_{Ba-L} infection of LCs within epithelial tissue, whereas MVC administration for either 3 or 14 days completely blocked LCs from *ex vivo* HIV_{Ba-L} infection (Figure 1). These data demonstrate the importance of the length of MVC dosing period before HIV exposure. MVC treatment also consistently prevented HIV_{Ba-L} transmission from LCs to cocultured CD4$^+$ T cells (Figure 2). Furthermore, MVC administration for 3 days blocked *ex vivo* virus infection of LCs as well as

subsequent virus transmission when different R5 HIV strains, HIV_{AD8} and HIV_{JR-FL}, were utilized for an additional six subjects ($n=3$ for each strain, Figures 1 and 2). These data demonstrate that oral administration of MVC for at least 3 days is capable of fully protecting HIV infection of LCs within epithelial tissue.

These experiments provide perhaps the best proof-of-concept test for MVC as a potential PrEP drug, as it would be unethical to expose MVC-treated volunteers to HIV *in vivo*. As proven here, orally delivered MVC rapidly distributes to skin and functionally acts to block infection of relevant target cells, LCs, supporting randomized controlled trials of MVC as a PrEP therapy for individuals at high risk of becoming infected with HIV through sexual exposure.

CONFLICT OF INTEREST

The authors state no conflict of interests.

ACKNOWLEDGMENTS

We thank Kazutoshi Harada and Naotaka Shibagaki for their helpful discussions, and Miyuki Ogino and Naoko Misawa for technical assistance. These studies were supported in part by a grant from the Ministry of Health Science of the Japanese Government (201029002).

Takamitsu Matsuzawa[1], Tatsuyoshi Kawamura[1], Youichi Ogawa[1], Masaaki Takahashi[2], Rui Aoki[1], Kohji Moriishi[3], Yoshio Koyanagi[4], Hiroyuki Gatanaga[5], Andrew Blauvelt[6] and Shinji Shimada[1]

[1]Department of Dermatology, Faculty of Medicine, University of Yamanashi, Yamanashi, Japan; [2]Department of Pharmacy, Nagoya Medical Center, Aichi, Japan; [3]Department of Microbiology, Faculty of Medicine, University of Yamanashi, Yamanashi, Japan; [4]Laboratory of Viral Pathogenesis, Institute for Virus Research, Kyoto University, Kyoto, Japan; [5]AIDS Clinical Center, National Center for Global Health and Medicine, Tokyo, Japan and [6]Oregon Medical Research Center, Portland, Oregon, USA
E-mail: tkawa@yamanashi.ac.jp

SUPPLEMENTARY MATERIAL

Supplementary material is linked to the online version of the paper at http://www.nature.com/jid

REFERENCES

Cohen MS, Chen YQ, McCauley M *et al.* (2011) Prevention of HIV-1 infection with early antiretroviral therapy. *N Engl J Med* 365:493–505

Dumond JB, Patterson KB, Pecha AL *et al.* (2009) Maraviroc concentrates in the cervicovaginal fluid and vaginal tissue of HIV-negative women. *J Acquir Immune Defic Syndr* 51:546–53

Ganor Y, Zhou Z, Tudor D *et al.* (2010) Within 1 h, HIV-1 uses viral synapses to enter efficiently the inner, but not outer, foreskin mucosa and engages Langerhans-T cell conjugates. *Mucosal Immunol* 3:506–22

Grant RM, Lama JR, Anderson PL *et al.* (2010) Preexposure chemoprophylaxis for HIV prevention in men who have sex with men. *N Engl J Med* 363:2587–99

Hu J, Gardner MB, Miller CJ (2000) Simian immunodeficiency virus rapidly penetrates the cervicovaginal mucosa after intravaginal inoculation and infects intraepithelial dendritic cells. *J Virol* 74:6087–95

Kawamura T, Bruse SE, Abraha A *et al.* (2004) PSC-RANTES blocks R5 human immunodeficiency virus infection of Langerhans cells isolated from individuals with a variety of CCR5 diplotypes. *J Virol* 78:7602–9

Kawamura T, Cohen SS, Borris DL *et al.* (2000) Candidate microbicides block HIV-1 infection of human immature Langerhans cells within epithelial tissue explants. *J Exp Med* 192:1491–500

Lederman MM, Offord RE, Hartley O (2006) Microbicides and other topical strategies to prevent vaginal transmission of HIV. *Nat Rev Immunol* 6:371–82

Ogawa Y, Kawamura T, Matsuzawa T *et al.* (2013) Antimicrobial Peptide LL-37 Produced by HSV-2-Infected Keratinocytes Enhances HIV Infection of Langerhans Cells. *Cell Host Microbe* 13:77–86

Patterson KB, Prince HA, Kraft E *et al.* (2011) Penetration of tenofovir and emtricitabine in mucosal tissues: implications for prevention of HIV-1 transmission. *Sci Transl Med* 3:112re4

Takahashi M, Hirano A, Okubo N *et al.* (2010) Development and application of a simple LC-MS method for the determination of plasma maraviroc concentrations. *J Med Invest* 57:245–50

van der Straten A, Van Damme L, Haberer JE *et al.* (2012) Unraveling the divergent results of pre-exposure prophylaxis trials for HIV prevention. *AIDS* 26:F13–9

Veazey RS, Ketas TJ, Dufour J *et al.* (2010) Protection of rhesus macaques from vaginal infection by vaginally delivered maraviroc, an inhibitor of HIV-1 entry via the CCR5 co-receptor. *J Infect Dis* 202:739–44

Veazey RS, Springer MS, Marx PA *et al.* (2005) Protection of macaques from vaginal SHIV challenge by an orally delivered CCR5 inhibitor. *Nat Med* 11:1293–4

Vaccine 31 (2013) 3199–3205

Contents lists available at SciVerse ScienceDirect

Vaccine

journal homepage: www.elsevier.com/locate/vaccine

Effects of immunization of pregnant guinea pigs with guinea pig cytomegalovirus glycoprotein B on viral spread in the placenta

Kaede Hashimoto[a,b], Souichi Yamada[a], Harutaka Katano[c], Saki Fukuchi[a,b], Yuko Sato[c], Minami Kato[a], Toyofumi Yamaguchi[d], Kohji Moriishi[b], Naoki Inoue[a,*]

[a] Department of Virology I, National Institute of Infectious Diseases, Tokyo, Japan
[b] Department of Microbiology, School of Medicine, University of Yamanashi, Yamanashi, Japan
[c] Department of Pathology, National Institute of Infectious Diseases, Tokyo, Japan
[d] Department of Biosciences, Teikyo University of Science, Yamanashi, Japan

ARTICLE INFO

Article history:
Received 5 March 2013
Accepted 24 April 2013
Available online 15 May 2013

Keywords:
Cytomegalovirus
Congenital infection
Animal model
Placenta
Glycoprotein B
Vaccine

ABSTRACT

Background: Cytomegalovirus (CMV) is the most common cause of congenital virus infection. Infection of guinea pigs with guinea pig CMV (GPCMV) can provide a useful model for the analysis of its pathogenesis as well as for the evaluation of vaccines. Although glycoprotein B (gB) vaccines have been reported to reduce the incidence and mortality of congenital infection in human clinical trials and guinea pig animal models, the mechanisms of protection remain unclear.
Methods: To understand the gB vaccine protection mechanisms, we analyzed the spread of challenged viruses in the placentas and fetuses of guinea pig dams immunized with recombinant adenoviruses expressing GPCMV gB and β-galactosidase, rAd-gB and rAd-LacZ, respectively.
Results: Mean body weight of the fetuses in the dams immunized with rAd-LacZ followed by GPCMV challenge 3 weeks after immunization was 78% of that observed for dams immunized with rAd-gB. Under conditions in which congenital infection occurred in 75% of fetuses in rAd-LacZ-immunized dams, only 13% of fetuses in rAd-gB-immunized dams were congenitally infected. The placentas were infected less frequently in the gB-immunized animals. In the placentas of the rAd-LacZ- and rAd-gB-immunized animals, CMV early antigens were detected mainly in the spongiotrophoblast layer. Focal localization of viral antigens in the spongiotrophoblast layer suggests cell-to-cell viral spread in the placenta. In spite of a similar level of antibodies against gB and avidity indices among fetuses in each gB-immunized dam, congenital infection was sometimes observed in a littermate fetus. In such infected fetuses, CMV spread to most organs.
Conclusions: Our results suggest that antibodies against gB protected against infection mainly at the interface of the placenta rather than from the placenta to the fetus. The development of strategies to block cell-to-cell viral spread in the placenta is, therefore, required for effective protection against congenital CMV infection.

© 2013 Elsevier Ltd. All rights reserved.

1. Introduction

Human cytomegalovirus (HCMV) is the most common cause of congenital virus infection. Congenital infection occurs in 0.2–1% of all births, and causes birth defects and developmental abnormalities, including sensorineural hearing loss (SNHL) and developmental delay [1–3]. Since one of the major routes of transmission to pregnant mothers is suggested to be *via* the excretions of their own children [4,5], development of a vaccine is the only effective way for protection against primary HCMV infection. Indeed, a review panel from the Institute of Medicine indicated that the development of a vaccine against HCMV, particularly with the aim of preventing primary infection in pregnant women, was of the highest priority among those for infectious diseases other than HIV [6]. As one of the promising approaches, purified glycoprotein B (gB) protein in combination with the MF59 adjuvant was used for a phase 2 clinical trial on CMV-seronegative women who had recently delivered a child and had intention of having another, and this subunit gB vaccine protocol demonstrated 50% efficacy against primary infection [7]. Although such results are encouraging, further studies are required to improve the efficacy and rapid waning of protection.

Animal models are generally valuable in gaining a better understanding of pathogenesis as well as in developing therapeutics for

* Corresponding author at: Laboratory of Herpesviruses, Department of Virology I, National Institute of Infectious Diseases, 1-23-1 Toyama, Shinjuku-ku, Tokyo 162-8640, Japan. Tel.: +81 3 4582 2663; fax: +81 3 5285 1180.
E-mail address: ninoue@nih.go.jp (N. Inoue).

0264-410X/$ – see front matter © 2013 Elsevier Ltd. All rights reserved.
http://dx.doi.org/10.1016/j.vaccine.2013.04.078

infectious diseases. In contrast to murine and rat CMVs, guinea pig CMV (GPCMV) crosses the placenta and causes infection *in utero*. Importantly, congenital GPCMV infection causes diseases similar to congenital HCMV diseases, such as IUGR and labyrinthitis [8–11]. Previous studies using a guinea pig model demonstrated that congenital infection and mortality in pups were reduced by the administration of anti-gB antibodies [12] or by immunization with gB in the form of a DNA or purified subunit vaccine [13,14]. In the placenta, GPCMV-induced histopathological lesions with viral antigens were localized at the transitional zone between the capillarized labyrinth and the noncapillarized interlobium [15]. However, the mechanism by which gB immunization inhibits such viral spread in the placenta and fetus remains unclear. In this study, to better understand the mechanism, we analyzed the spread of viruses in the placentas and fetuses of gB-immunized dams after virus challenge.

2. Materials and methods

2.1. Cells and viruses

Guinea pig lung fibroblasts (GPL, ATCC) were initially cultured in F-12 medium supplemented with 10% fetal bovine serum (FBS) and subsequently, after infection with GPCMV, in F-12 medium supplemented with 2% FBS. GPL cells were infected with a GPCMV (strain 22122) stock purchased from ATCC. Salivary glands (SGs) of a guinea pig (Hartley strain) infected with the original GPCMV stock were recovered, minced, sonicated briefly, and then centrifuged to remove debris. The supernatant (SG-P0) was used for the infection of GPL cells, and viral stocks were prepared after propagation of the cell-free virus 5 times in GPL cells (SG-P5). Virus stocks were concentrated by ultracentrifugation (82,000 × *g* for 2 h) in a 20% sucrose step gradient. Infectious units (IUs) of the stocks were determined by immunostaining of GPL cells infected with the diluted stocks in 12- or 24-well plates and cultured for 2–3 days as described previously [16].

A recombinant GPCMV expressing red fluorescent protein (RFP) was prepared as follows: The sequence region from position 4244 to 8013 (positions are based on Ref. [17]) of GPCMV (SG-P5) was replaced with a 1.8-kb DNA fragment covering the TurboRFP gene under the control of the CMV IE promoter (Evorgen JSC, Russia) by homologous recombination in GPL cells. The RFP-expressing GPCMV candidates were then plaque-purified several times in GPL cells. One of the candidates, GPCMV-RFP(4A), was used for neutralization assay.

2.2. Recombinant adenoviral vectors

The gene encoding the extracellular domain (amino acids 1–674) of GPCMV gB (rAd-gB) and the LacZ gene encoding β-galactosidase were cloned into a pENTR-3C vector and then into pAd/CMV/V5/DEST by using the LR recombinase system (Invitrogen), resulting in pAd-gB and pAd-LacZ, respectively. Recombinant adenoviruses, rAd-gB and rAd-LacZ, were recovered by transfection of 293A cells with pAd-gB and with pAd-LacZ, respectively, amplified, and purified by centrifugation through two CsCl step gradients as described previously [18].

2.3. Animal studies

Female guinea pigs at the indicated weeks after birth (Hartley, Japan SLC, Inc.) were inoculated intraperitonealy (i.p.) with 10^6 IUs of GPCMV and euthanized 3-weeks later. Blood specimens were drawn directly from the heart, and organ specimens, including liver, spleen, kidney, lung, and salivary gland, were harvested. Dams at 1-week of gestation (Japan SLC, Inc.) were inoculated i.p. with 10^{10} transducing units (TUs) of rAd viruses, infected subcutaneously with 10^6 IUs of GPCMV (SG-P5) 3-weeks after the inoculation, and euthanized 3-weeks later. Blood specimens were drawn from the dams and their fetuses. Salivary glands were also obtained from the dams. The placentas and fetuses were weighed and organs were harvested from the fetuses. All animal procedures were approved by the Animal Care and Use Committee of the National Institute of Infectious Diseases (NIID), and were conducted according to the 'Guidelines for Animal Experiments Performed at the NIID'.

2.4. Immunological assays

Transfection was performed by using a commercial reagent (Fugene6, Roche). GPCMV-infected and -transfected cells were fixed with acetone for 5 min and expression of antigens were examined by an immunofluorescence assay as described previously [19].

Anti-gB antibody levels in the dams and fetuses were measured by ELISA using the cytoplasmic fraction (0.8 μg of protein/well) of 293T cells transfected with a gB construct. Absorbance values obtained using sera diluted at 1:200 had a good correlation with titers determined as a maximum dilution (in a range of 1:200–3200) that gives the threshold absorbance (data not shown). Avidity indices of anti-gB IgG were determined by a 10-min treatment with 4 M urea.

Neutralizing activities in sera were measured as follows. A total of 1×10^4 IUs of GPCMV-RFP(4A) in 50 μl of medium was mixed with 50 μl of serially diluted serum specimens, and incubated at 37 °C for 1 h. The reaction mixtures were then diluted and inoculated into GPL cell cultures. RFP-positive foci were counted 3 days after infection.

2.5. Immunohistochemistry

All organs obtained from sacrificed animals were fixed in 10% buffered formalin. Formalin-fixed specimens were embedded in paraffin, sectioned, and stained with hematoxylin and eosin (HE), as described previously [8]. Immunohistochemical analysis was performed using the monoclonal antibody g-1, which detects a GPCMV early antigen, or the rabbit polyclonal antibody against immediate-early proteins 1 and 2, which was generated by the immunization of rabbits with a GST-IE1/2 fusion protein, as primary antibodies. For the second- and third-phase immunostaining reagents, a biotinylated $F(ab')_2$ fragment of rabbit anti-mouse immunoglobulin (DAKO) or of goat anti-rabbit immunoglobulin (DAKO) and peroxidase-conjugated streptavidin (DAKO) were used. DAB was used as a chromogen and the slides were counterstained with hematoxylin.

2.6. Quantification of viral DNA

DNA samples were prepared from the placentas and fetal organs, and viral DNAs in the samples were detected by real-time PCR assays for GPCMV GP83 and β-actin genes as described previously [16].

2.7. Statistical analysis

Mann–Whitney *U* test was used to analyze statistical differences in the weight of animals, fetuses, and placentas, and in the number of viral foci in placentas. Chi-square test was also used to analyze differences in the rates of CMV-positive placentas and fetal organs.

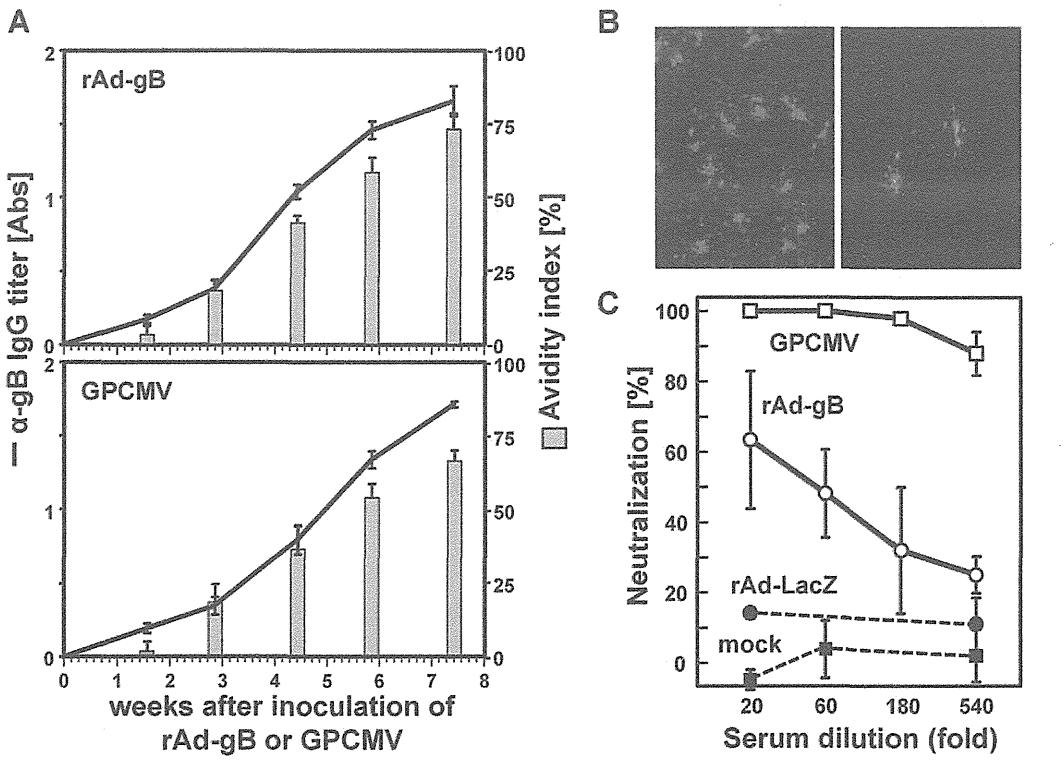

Fig. 1. Induction of anti-gB antibodies by immunization with rAd-gB. (A) Three 4-week old guinea pigs were inoculated with 10^{10} TUs of rAd-gB and GPCMV, respectively. Blood specimens were drawn from the great saphenous vein at the indicated days after inoculation, and their anti-gB IgG titers and avidity indices were measured. (B) RFP-expressing GPCMV, GPCMV-RFP(4A), was used for the detection of neutralizing antibodies. Examples of RFP foci detected in GPL cells after treatment of the virus with sera obtained from the mock-infected (left) and GPCMV-infected (right) animals are shown. (C) Neutralization assay was performed at indicated serum dilutions in triplicate. Serum specimens obtained from 3 guinea pigs immunized with rAd-gB and rAd-LacZ 7-weeks after immunization were analyzed and the averages and SDs of neutralization (%) by the respective 3 specimens are plotted. No reduction and complete inhibition of RFP-positive foci are indicated as 0% and 100% neutralization, respectively. Sera obtained from mock- and GPCMV-infected guinea pigs were used as negative and positive controls, respectively, for the detection of neutralizing antibodies.

3. Results

3.1. gB immunization of young animals

Administration of 10^{10} TUs of rAd-gB to young guinea pigs induced anti-gB antibodies, and the avidity index for the anti-gB antibodies increased gradually (Fig. 1A). Neutralizing activities against GPCMV in sera were measured by using RFP-expressing GPCMV (Fig. 1B and C). Although the anti-gB IgG titers and avidity indices of sera obtained from the animals immunized with rAd-gB were at a level similar to those of sera obtained from the animals infected with GPCMV (SG-P5), the neutralizing activities of the former sera were weaker than those of the latter sera, suggesting the presence of neutralizing antibodies other than those against gB.

Next, young animals were inoculated with rAd-gB or rAd-LacZ, and challenged with GPCMV at 2- to 4-weeks after inoculation. Although the GPCMV challenge resulted in a short-term weight loss of 6–17% in the rAd-LacZ-inoculated control animals, gB immunization suppressed weight loss (Fig. 2). It seems that younger animals are more prone to body weight loss after virus challenge. In addition, the amount of viral DNA in the salivary glands in the rAd-gB-inoculated animals was less than 1% that in the rAd-LacZ-inoculated animals (data not shown), indicating that gB immunization reduced viral dissemination to the salivary glands.

3.2. Protection of the placentas and fetuses against infection in gB-immunized dams

We observed that viral antigens and DNA were rarely detected in the placenta 1-week after infection at 4-weeks of gestation, but

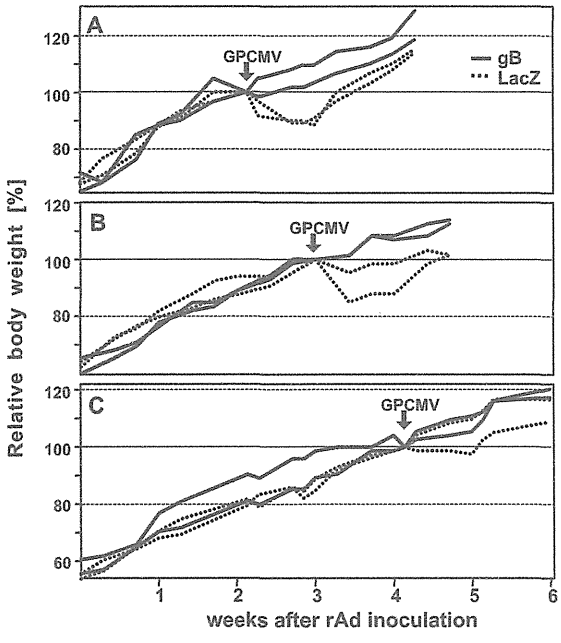

Fig. 2. Relative body weights of animals immunized with rAd-gB (continuous lines) and with rAd-LacZ (dashed lines) followed by GPCMV challenge (arrows) at 2-weeks (A), 3-weeks (B) and 4-weeks (C) after immunization are shown by using the weight of each animal at the time of the challenge as a 100% control.

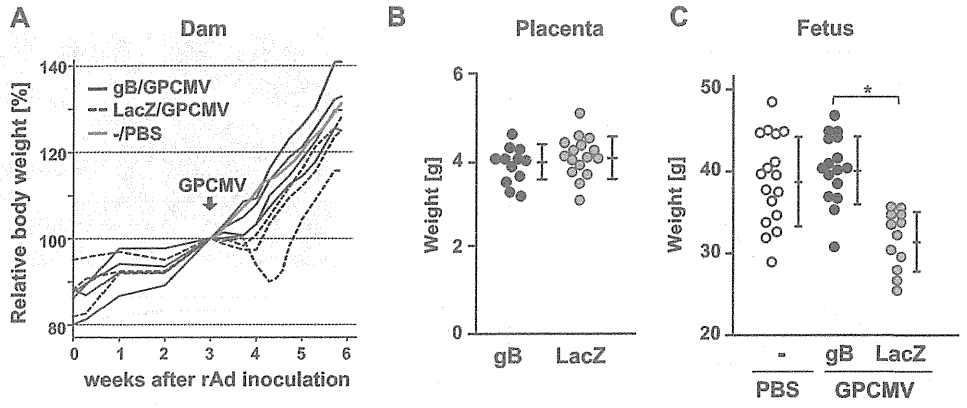

Fig. 3. (A) Relative body weights of dams immunized with rAd-gB (continuous lines), with rAd-LacZ (dashed lines), and with PBS (gray) followed by GPCMV challenge (arrow) are shown by using the body weight of each animal at the time of the GPCMV challenge (arrows) as a 100% control. Comparison of weights of the placentas (B) and fetuses (C) from dams without any treatment (open circles) and from dams immunized with rAd-gB (closed circles) or rAd-LacZ (gray circles). Each circle indicates one placenta or fetus. Means and SDs are shown. An asterisk means $p < 0.01$.

became detectable by 3-weeks after infection irrespective of the gestational age of the dams (data not shown). Based on this observation, we designed the experimental schedule as follows: guinea pigs were inoculated with 10^{10} TUs of Ad-LacZ or Ad-gB at 1-week of gestation, infected subcutaneously with 10^6 IUs of GPCMV at 4-weeks of gestation, and then sacrificed at 7-weeks of gestation. Although there was no difference in weight between the placentas from the gB- and LacZ-immunized dams, there was a significant difference in weight between the fetuses from the gB-immunized dams and those from the LacZ-immunized dams (Fig. 3). Taking the mean and standard deviation (SD) of the weight of the fetuses from untreated dams as the standard, we found that 42% of the fetuses from the LacZ-immunized dams exhibited IUGR, which was defined as a fetal weight less than the mean–1.5SD, whereas none of those from the gB-immunized dams did. Viral DNAs were detected by PCR in 75% and 13% of the fetuses from the LacZ- and gB-immunized dams, respectively (Fig. 4A). Two out of 16 fetuses from the gB-immunized dams (#A-1 and #B-5) were GPCMV positive. GPCMV DNAs were detected in most of their organs, and the viral loads in each organ were comparable to those from the LacZ-immunized dams (Fig. 4B).

3.3. Serological observations after challenge

Anti-gB antibody titers in the fetuses from the gB-immunized dams were similar to those of the dams (Fig. 5A). This was also true for the avidity indices against anti-gB IgG (Fig. 5B). As compared with the dams inoculated with rAd-LacZ, the anti-gB antibody titers and the avidity indices were significantly higher in the dams inoculated with rAd-gB, suggesting the presence of efficient pre-existing immunity in the dams immunized with rAd-gB.

No differences in weight in the placentas or fetuses, in the anti-gB IgG levels, or in the avidity indices (data not shown) were observed among the littermates of the gB-immunized dam A (#1–#4) as well as among those of dam B (#5–#8), suggesting

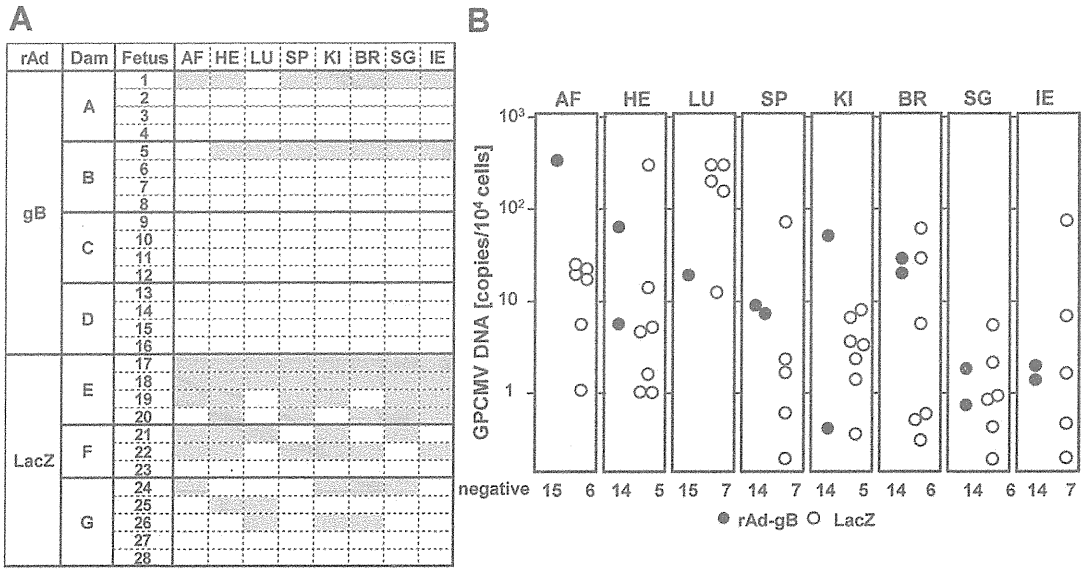

Fig. 4. GPCMV DNA detected in the organs of fetuses from dams immunized rAd-gB or -LacZ. (A) Shaded boxes indicate the presence of GPCMV DNA. (B) Viral loads (GPCMV DNA copies per 10^4 cells) of the organs from the fetuses are plotted. AF: amnion fluid, HE: heart, LU: lung, SP: spleen, KI: kidney, BR: brain, SG: salivary gland, and IE: inner ear.

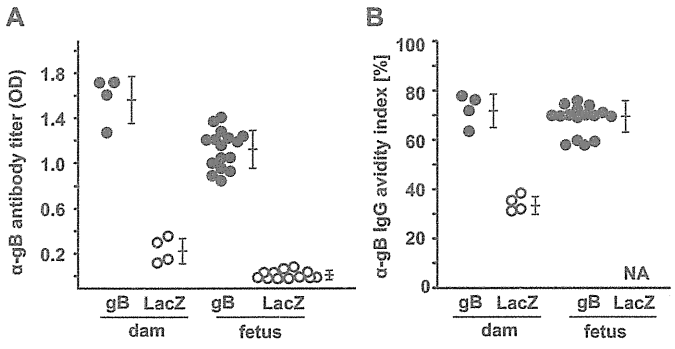

Fig. 5. Comparison of the anti-gB IgG titers and avidity indices against gB in sera obtained from dams immunized with rAd-gB (closed circles) or rAd-LacZ (open circles) and in sera from the fetuses. Each circle indicates one dam or fetus. Means and SDs are shown.

that gB-immunization protects the fetuses from IUGR irrespective of congenital infection and that the presence of anti-gB antibodies in the fetuses is not a sufficient determinant for protection from congenital infection.

3.4. Localization of GPCMV antigens in the placenta from gB-immunized dams

Immunohistochemical analysis using the anti-GPCMV monoclonal antibody g-1, which recognizes a 50-kDa viral protein expressed during the early phase of infection, showed that viral antigens were present focally in the placentas. In experiment A, in which the placenta specimens indicated in Figs. 3–5 were analyzed, 5 out of the 16 placentas from the gB-immunized dams were CMV positive, while 8 out of the 12 placentas from the LacZ-immunized dams were positive (Fig. 6B). The use of polyclonal antibodies against the IE2 protein gave similar results (data not shown). Taking into account the number of foci per slice, we found that more viral antigens were detected in the placentas of the LacZ-immunized dams ($p < 0.05$). However, as the difference was small, an additional set of dams were analyzed in the same way (experiment B), with similar results obtained in those animals. A comparison of CMV-positive rates in the placentas from gB- and LacZ-immunized dams in the combined results from experiments A and B revealed a statistical significance ($p < 0.05$), indicating the gB-immunization reduced CMV infection in the placentas. In the placentas from the dams immunized with rAd-LacZ, viral antigens

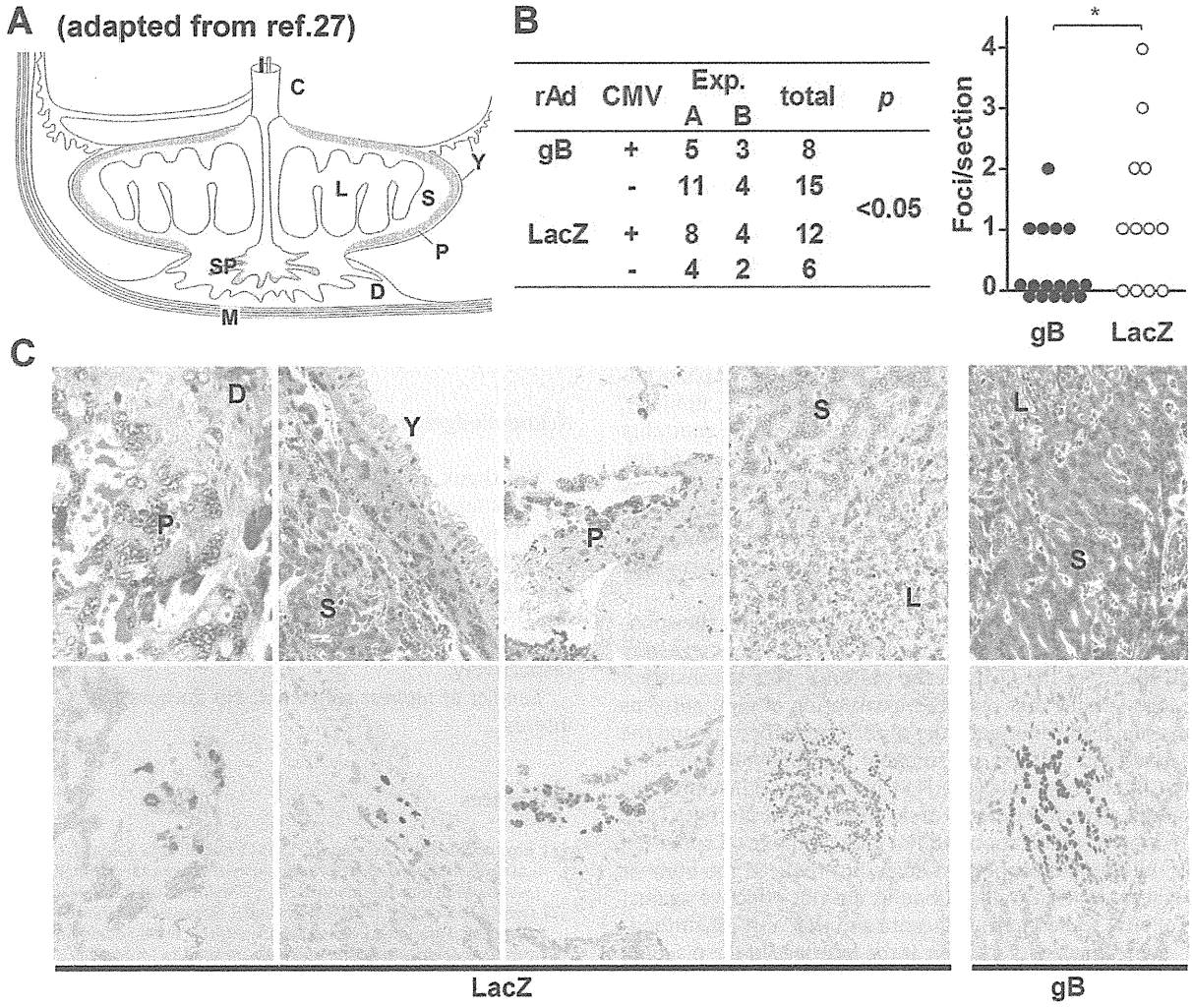

Fig. 6. Detection of viral antigens in the placentas. (A) Schematic presentation of the placental structure of guinea pigs (adapted from Ref. [27]). C: cord, M: myometrium, D: decidua, SP: subplacenta, Y: visceral yolk sac, P: parietal yolk sac, S: spongiotrophoblast layer, and L: labyrinth. (B) Numbers of CMV-positive foci in the placentas from rAd-gB- and rAd-LacZ-immunized dams. Two experiments, A and B, were performed. In the experiments (Exp.) A and B, the placenta specimens indicated in Figs. 3–5 and those obtained from an additional set of immunized dams were analyzed. A comparison of the number of foci per section in the placentas from dams immunized with rAd-gB (closed circles) or rAd-LacZ (open circles) in Exp. A is shown. An asterisk represents $p < 0.05$. (C) Localization of viral antigens in the placenta. HE staining (upper panels) and immunohistochemistry with anti-GPCMV antibody g-1 (lower panels) are shown.

were mainly detected in the spongiotrophoblast layer, occasionally in trophoblast giant cells in the parietal yolk sac, and only sporadically in the visceral yolk sac (Fig. 6C). No destruction of the spongy structure or inflammation was observed in the spongiotrophoblast layer. In contrast, some structural destruction and inclusion bodies were occasionally observed in the yolk sac. In the gB-immunized dams, viral antigens were detected only in the spongiotrophoblast layer. However, there was no apparent difference in the size of the CMV-positive foci in the spongiotrophoblast layer between the rAd-gB- and rAd-LacZ-immunized groups.

4. Discussion

Guinea pig models have been used for many years in an attempt to clarify the pathogenesis of congenital CMV infection. However, most prior studies using the guinea pig model for vaccine studies have focused on infection in pups. Since guinea pigs consume the placentas after delivery, there is little information on how CMV spreads in the placentas and then into the fetuses and on how gB vaccination prevents viral spread to and in the placenta. In addition, most prior studies used sera obtained from GPCMV-infected animals; in other words, sera in which active infection cannot be distinguished from abortive infection. Thus, our study is unique in undertaking the precise analysis of viral spread in placentas using a well-characterized monoclonal antibody. The most important findings in this study are as follows: (i) immunization of dams with gB reduced the level of viral antigens in the placentas slightly, but significantly, (ii) this slight reduction in viral load resulted in marked differences in the rates of IUGR (42% *vs.* 0%) and congenital infection (75% *vs.* 13%), (iii) gB immunization did not inhibit focal virus growth in the placentas, and (iv) the presence of anti-gB antibodies in the fetuses did not protect against viral spread in the fetuses.

Schleiss et al. demonstrated that preconceptional immunization with purified gB in combination with Freund's adjuvant reduced both pup mortality to 14% and CMV-infection in liveborn pups to 22% *vs.* 76% and 50%, respectively, in the unvaccinated group [13], and that a DNA vaccine expressing gB did not improve pup mortality but reduced the rate of viral transmission by half [14]. Similarly, immunization with GPCMV glycoproteins reduced pup mortality to 14% *vs.* 56% in the unvaccinated group [20]. The absence of any difference in the birth weight of pups born from dams with and without immunization is thought to be due to their comparison of the weights of only liveborn pups. The rate of congenital infection and the efficacy of gB immunization in our study were generally consistent with the results observed in those studies.

GPCMV infection in the placenta occurred focally in the spongiotrophoblast layer at a relatively low frequency, suggesting cell-to-cell spread of the virus in the placenta. This is consistent with previous studies that reported localization of viral antigens at the transitional zone between the capillarized labyrinth and the noncapillarized interlobium, presumably the spongiotrophoblast layer, with GPCMV-related lesions [15]. In humans, HCMV proteins have also been detected in focal areas in the term placenta [21]. The fact that gB immunization did not change the focal spread of GPCMV in the spongiotrophoblast layer, but reduced the number of foci, suggests that anti-gB antibodies are not effective against this form of viral spread in the placenta and that anti-gB antibodies mainly protect against infection at the interface of the placenta rather than inside the placenta or from the placenta to the fetus.

Recent studies on HCMV have demonstrated that human sera obtained from individuals naturally infected, but not from those immunized with the gB subunit vaccine or with the attenuated strain Towne, contain strong neutralizing activities against infection to endothelial and epithelial cells [22]. HCMV entry into endothelial cells can be inhibited with antibodies against UL128, UL130 and UL131A [23]. Since the major cell types comprising the placenta are cytotrophoblasts and syncytotrophoblasts, both of which possess similarities to epithelial cells, and vascular endothelial cells, it is plausible that neutralizing antibodies against gB cannot efficiently inhibit viral spread in the placenta. The neonatal Fc receptor mediated-transcytosis of CMV virions has been proposed as one possible mechanism for viral dissemination in the placenta, thus highlighting the importance of the quality and quantity of CMV-specific neutralizing antibodies to the prevention of viral transmission to the fetus [24]. It would be interesting to see whether immunization with the gH/gL/UL128/UL130/UL131A pentamer complex could protect the placenta against CMV infection. Although we tried to induce antibodies against GPCMV GP131, the HCMV UL130 homolog, by using the same rAd system, we could not induce a high level of anti-GP131 antibodies (data not shown).

The significant rate of IUGR observed in spite of the limited viral activity in the placenta suggests that infection induces secondary effects on placental functions. It would be important to identify which of the cellular genes are affected by CMV infection in the placenta. A recent study on amnion fluid specimens from pregnant women with congenital HCMV infection demonstrated that HCMV infection during pregnancy was associated with a shift in cytokine expression toward a proinflammatory state [25]. Pathological analyses on the placentas from women with congenital infection indicated that vascular endothelial growth factor (VEGF) and its receptor, fms-like tyrosine kinase 1 (Flt1), were up-regulated, and the amniotic fluid contained elevated levels of soluble Flt1 (sFlt1), an antiangiogenic protein, relative to placental growth factor. Hyperimmune globulin treatment reduced both VEGF and Flt1 expression as well as the sFlt1 levels [26]. Microarray analyses of cellular gene expression in the placentas of GPCMV-infected guinea pigs are currently under way.

In conclusion, this study demonstrated that a slight reduction in placental infection by immunization with gB can result in a significant prevention of IUGR and congenital infection, and that gB immunization may not be effective in reducing viral spread in the placenta.

Acknowledgements

We thank Yoshiko Fukui and Mihoko Tsuda for their technical assistance and Yoshihiro Tsutsui for the monoclonal antibody g-1. This work was supported by the following grants: Grant on Research on Health Sciences focusing on Drug Innovation (SHC4401) from Japanese Human Science Foundation to NI and HK, and Grants-in-Aid for Scientific Research C and for Young Scientists B from the Japan Society for the Promotion of Science to NI and SY, respectively.

Conflict of interest statement: No authors have any conflict of interest.

References

[1] Koyano S, Inoue N, Nagamori T, Yan H, Asanuma H, Yagyu K, et al. Dried umbilical cords in the retrospective diagnosis of congenital cytomegalovirus infection as a cause of developmental delays. Clin Infect Dis 2009;48:e93–5.
[2] Ogawa H, Suzutani T, Baba Y, Koyano S, Nozawa N, Ishibashi K, et al. Etiology of severe sensorineural hearing loss in children: independent impact of congenital cytomegalovirus infection and GJB2 mutations. J Infect Dis 2007;195:782–8.
[3] Pass RF. Cytomegalovirus. In: Knipe DM, Howley PM, editors. Fields virology. 4th ed. Philadelphia, PA: Lippincott Williams & Wilkins; 2001. p. 2675–705.
[4] Koyano S, Inoue N, Oka A, Moriuchi H, Asano K, Ito Y, et al. Screening for congenital cytomegalovirus infection using newborn urine samples collected on filter paper: feasibility and outcomes from a multicentre study. BMJ Open 2011;1:e000118.
[5] Fowler KB, Pass RF. Risk factors for congenital cytomegalovirus infection in the offspring of young women: exposure to young children and recent onset of sexual activity. Pediatrics 2006;118:e286–92.

[6] Stratton KR, Durch JS, Lawrence RS. Vaccines for the 21st century. Washington, DC: National Academy Press; 2000.
[7] Pass RF, Zhang C, Evans A, Simpson T, Andrews W, Huang ML, et al. Vaccine prevention of maternal cytomegalovirus infection. N Engl J Med 2009;360:1191–9.
[8] Katano H, Sato Y, Tsutsui Y, Sata T, Maeda A, Nozawa N, et al. Pathogenesis of cytomegalovirus-associated labyrinthitis in a guinea pig model. Microbes Infect 2007;9:183–91.
[9] Park AH, Gifford T, Schleiss MR, Dahlstrom L, Chase S, McGill L, et al. Development of cytomegalovirus-mediated sensorineural hearing loss in a Guinea pig model. Arch Otolaryngol Head Neck Surg 2010;136:48–53.
[10] Woolf NK, Koehrn FJ, Harris JP, Richman DD. Congenital cytomegalovirus labyrinthitis and sensorineural hearing loss in guinea pigs. J Infect Dis 1989;160:929–37.
[11] Griffith BP, Lucia HL, Hsiung GD. Brain and visceral involvement during congenital cytomegalovirus infection of guinea pigs. Pediatr Res 1982;16:455–9.
[12] Chatterjee A, Harrison CJ, Britt WJ, Bewtra C. Modification of maternal and congenital cytomegalovirus infection by anti-glycoprotein b antibody transfer in guinea pigs. J Infect Dis 2001;183:1547–53.
[13] Schleiss MR, Bourne N, Stroup G, Bravo FJ, Jensen NJ, Bernstein DI. Protection against congenital cytomegalovirus infection and disease in guinea pigs, conferred by a purified recombinant glycoprotein B vaccine. J Infect Dis 2004;189:1374–81.
[14] Schleiss MR, Bourne N, Bernstein DI. Preconception vaccination with a glycoprotein B (gB) DNA vaccine protects against cytomegalovirus (CMV) transmission in the guinea pig model of congenital CMV infection. J Infect Dis 2003;188:1868–74.
[15] Griffith BP, McCormick SR, Fong CK, Lavallee JT, Lucia HL, Goff E. The placenta as a site of cytomegalovirus infection in guinea pigs. J Virol 1985;55:402–9.
[16] Nozawa N, Yamamoto Y, Fukui Y, Katano H, Tsutsui Y, Sato Y, et al. Identification of a 1.6 kb genome locus of guinea pig cytomegalovirus required for efficient viral growth in animals but not in cell culture. Virology 2008;379:45–54.
[17] Kanai K, Yamada S, Yamamoto Y, Fukui Y, Kurane I, Inoue N. Re-evaluation of the genome sequence of guinea pig cytomegalovirus. J Gen Virol 2011;92:1005–20.
[18] Kanegae Y, Makimura M, Saito I. A simple and efficient method for purification of infectious recombinant adenovirus. Jpn J Med Sci Biol 1994;47:157–66.
[19] Yamada S, Nozawa N, Katano H, Fukui Y, Tsuda M, Tsutsui Y, et al. Characterization of the guinea pig cytomegalovirus genome locus that encodes homologs of human cytomegalovirus major immediate-early genes, UL128, and UL130. Virology 2009;391:99–106.
[20] Bourne N, Schleiss MR, Bravo FJ, Bernstein DI. Preconception immunization with a cytomegalovirus (CMV) glycoprotein vaccine improves pregnancy outcome in a guinea pig model of congenital CMV infection. J Infect Dis 2001;183:59–64.
[21] McDonagh S, Maidji E, Chang HT, Pereira L. Patterns of human cytomegalovirus infection in term placentas: a preliminary analysis. J Clin Virol 2006;35:210–5.
[22] Cui X, Meza BP, Adler SP, McVoy MA. Cytomegalovirus vaccines fail to induce epithelial entry neutralizing antibodies comparable to natural infection. Vaccine 2008;26:5760–6.
[23] Gerna G, Sarasini A, Patrone M, Percivalle E, Fiorina L, Campanini G, et al. Human cytomegalovirus serum neutralizing antibodies block virus infection of endothelial/epithelial cells, but not fibroblasts, early during primary infection. J Gen Virol 2008;89:853–65.
[24] Maidji E, McDonagh S, Genbacev O, Tabata T, Pereira L. Maternal antibodies enhance or prevent cytomegalovirus infection in the placenta by neonatal Fc receptor-mediated transcytosis. Am J Pathol 2006;168:1210–26.
[25] Scott GM, Chow SS, Craig ME, Pang CN, Hall B, Wilkins MR, et al. Cytomegalovirus infection during pregnancy with maternofetal transmission induces a proinflammatory cytokine bias in placenta and amniotic fluid. J Infect Dis 2012;205:1305–10.
[26] Maidji E, Nigro G, Tabata T, McDonagh S, Nozawa N, Shiboski S, et al. Antibody treatment promotes compensation for human cytomegalovirus-induced pathogenesis and a hypoxia-like condition in placentas with congenital infection. Am J Pathol 2010;177:1298–310.
[27] Kaufmann P, Davidoff M. The guinea-pig placenta. Adv Anat Embryol Cell Biol 1977;53:5–91.